SEVEN
publicações acadêmicas

Using satellite images to identify heat islands in city of Ilha Solteira – SP

https://doi.org/10.56238/interdiinovationscrese-070

Lucas Barbosa Nishigima
Paulista State University "Júlio de Mesquita Filho"
Engineering College
Ilha Solteira Campus

Helio Ricardo Silva
Prof. Dr., Paulista State University "Júlio de Mesquita Filho"
Engineering College
Ilha Solteira Campus

ABSTRACT
With population growth, it is necessary to increase the number of constructions, such as residences, asphalt. With that comes the consequences, because when we have agglomerations of houses there is a lot of absorption of solar rays causing the Urban Heat Islands (ICU) that tend to cause thermal discomfort for the population since there is an increase in temperature in that place. Remote Sensing comes as a solution to identify where the Heat Islands are and with that, we can plan ways to reduce them. This phenomenon was studied in this present work using LandSat-8 satellite images from the years 2018, 2019, 2020 and 2021 in the thermal infrared region (TIRS/LandSat-8) using the free software QGis 3.16 to process the images and determine the temperature of surface, climatological studies were also carried out to find out if there was influence on the formation of Urban Heat Islands in the city of Ilha Solteira. In general, the years 2018 and 2019 were the years with the highest incidence of Heat Islands.

Keywords: Remote Sensing, Thermal Infrared, Climatology, Surface Temperature.

1 INTRODUCTION

According to the Population Reference Bureau (PRB), the planetary population reached, at the end of 2020, about 7 billion and 800 million inhabitants. Of this total, approximately 55% live in cities, according to data published by the United Nations (UN) in 2019. Currently, about 85% of the Brazilian population lives in urbanized spaces (IBGE, 2017), whether metropolitan cities or cities in the countryside, large, medium or small cities. Urban heat islands (ICU's) are phenomena characterized by warmer temperatures in urban regions compared to the rural environments in their surroundings (ROTH, 2013).

According to Gartland (2010 p.09), the ICU's "... are formed in urban and suburban areas because many common building materials absorb and retain more heat from the soil than natural materials in less urbanized rural areas" and this is proven in other work already carried out.

Among the main impacts caused by urbanization, the reduction of green areas stands out, which are replaced by synthetic materials (mainly asphalt and concrete) used in construction and paving (HU & JIA, 2010).

According to (PORANGABA and AMORIM, 2019), the intensification of intra-urban temperature in relation to the nearby rural environment is worrisome because it directly influences people's lives, whether due to thermal discomfort or health-related issues.

Remote sensors are best suited to assess daytime UCI as they capture the temperature and other physical characteristics (such as albedo and emissivity) of a set of heterogeneous surfaces within the urban area, such as roof, vegetation, pavement, exposed soil and water bodies, from the spectral response of these surfaces (GAMARRA et al., 2013).

The objective of this work was to identify urban heat islands in a small municipality, Ilha Solteira – SP, verifying the relationship of their occurrences associated with climatological data.

2 LITERATURE REVIEW

2.1 URBANIZATION AND CLIMATOLOGICAL EFFECTS

Urbanization is a pertinent process in the history of human beings. Initially, this process occurred on a small scale, as a way of protecting the external environment, and recently, it has become increasingly necessary, since human activities have become more susceptible to the adversities of nature, such as intense rains and prolonged droughts (KEGLER; WOLLMANN; BANDEIRA, 2017).

Migration from the countryside to the city is a permanent phenomenon in history. Data from the Demographic Census conducted by the Brazilian Institute of Geography and Statistics in 2010 (IBGE, 2010) show a continuous migration of rural populations to cities in Brazil. Corroborating this information, the Population Bulletin (2007) shows that about 50% of the world's population is concentrated in urban areas and this number tends to become increasingly larger.

LIMA (2012) states that the growth of cities, together with that of urban populations, introduces new physical and chemical elements into the atmosphere, altering the previous natural conditions and giving rise to the urban climate. This statement corroborates SANTANA (2014), where the climate of cities are the most affected by climatic anomalies.

The differences in intra-urban surface temperature in relation to the nearby rural environment form the urban climate and heat islands (PORANGABA and AMORIM, 2019) and which, according to (Jensen, 2009, p. 288), "are caused by deforestation and replacement of the soil surface by non-evaporative and non-porous materials, such as asphalt and concrete".

According to Ribeiro et al. (2016) "the study of climate change caused by urbanization gained momentum with a more vigorous urbanization, from the mid-twentieth century onwards, and with the expansion of the size of cities".

The Center for Disease Control and Prevention (CDC) recorded that in the period from 1979 to 2003, exposure to excessive heat contributed to 3,442 premature deaths in the United States (CDC, 2016)

It is estimated that by 2045, about two billion more people will seek out cities to live in (The World Bank, 2016)

Among the urbanization characteristics that contribute to the development of ICU, geometry (KRUGER et al., 2011) stands out, which refers to the dimensions and spacing of buildings within the city, which affects wind flow, energy absorption, and the ability of the surface to emit long-wave radiation into space (COSTA, et al., 2010).

Among the problems visualized in the urban space, social problems stand out, such as the issue of housing, slums, occupation of riverside areas and/or lakes, etc., such issues sometimes lead to environmental problems such as floods, deforestation, silting of water sources, air and water pollution, etc. I also highlight the changes that are taking place in the city and that affect the quality of life in the climatic context, such as the use of concrete, verticalization, the preference for construction materials that absorb heat, the reduction of parks and green areas, the exacerbated emission of pollutants by automobiles and industries, etc.

The heat island effect is more intense on calm, clear days, since more solar energy is captured on clear days, and milder winds remove heat more slowly, causing the heat island to become more intense (GARTLAND, 2010).

2.2 HEAT ISLANDS

Heat islands are usually caused by human interference, such as the construction of houses, buildings, asphalt, deforestation, and erosion by land set-off. According to MASHIKI (2012), UCI is a phenomenon resulting from the energy balance in the urban space, which is characterized by the accumulation of heat on surfaces and consequent increase in air temperature. It's a "reverse oasis" where the air and surface temperatures are warmer than in surrounding rural areas. (GARTLAND, 2010).

According to García (1996), the classification of heat islands varies from: weak magnitude when the differences between the points oscillate between 0° and 2° C, medium magnitude between 2° and 4° C, strong between 4° and 6° C and very strong when the differences exceed 6º C. In the municipality of Ilha Solteira, Costa *et al.* (2010), found a temperature range of up to 7°C in the summer season.

According to NAKATA-OSAKI et al. (2016), air and surface temperatures in urban areas tend to be higher than temperatures in surrounding rural areas, due to urbanization characteristics such as air pollution, anthropogenic heat, impermeable surfaces, thermal properties of materials, and surface geometry (Figure 1). Atmospheric heat islands are, therefore, defined as pockets of warm air recorded in urban environments resulting from the differentiated capacity of materials found on the surface to store and reflect solar energy and the production of anthropogenic heat. They result from the

differences in the energy balance between the urban and rural areas, in addition to the differences within the city itself (AMORIM, 2017). The main causes of the urban heat island of the lower urban atmosphere are: urban geometry, air pollution, heat emission from buildings, traffic and metabolism of living organisms, land cover and building materials (BARROS et al., 2012), as shown in Figure 1.

Figure 1: Heat Island Profile

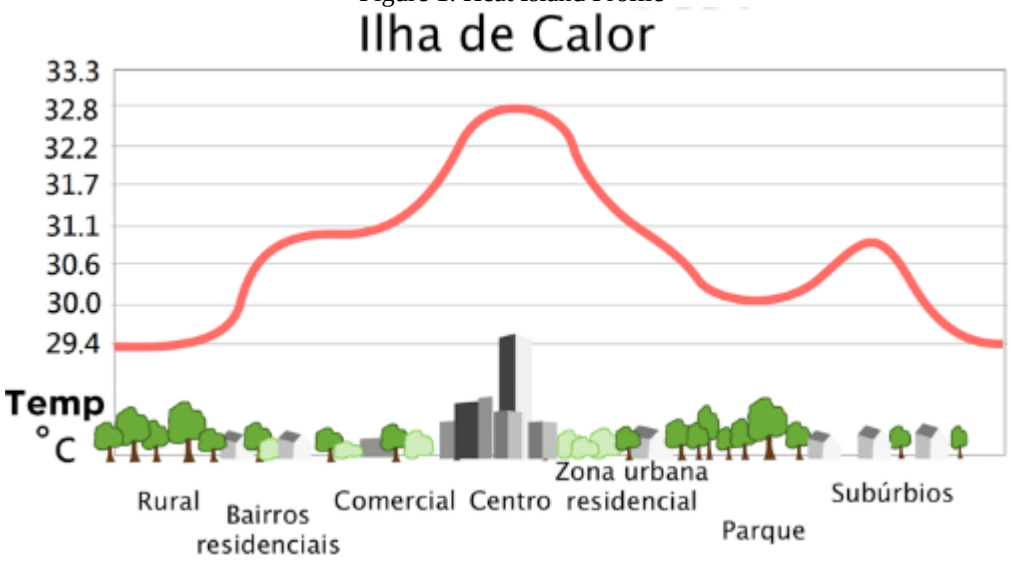

Source: EPA, 2016

2.3 GEOTECHNOLOGIES

With the creation and launch of several satellites in recent decades, many of the urban climate studies have been carried out based on remote sensing. The use of such techniques has contributed to the notoriety of studies of heat islands and thermal anomalies (BARBOSA & VECCHIA, 2009)

Most remote sensors record the electromagnetic radiation reflected or emitted by the targets, but depending on the purpose of the application, they can also record other types of energy, such as thermal energy (NISHIDA, 1998). Thermal-type energy captures the surface temperature of the upper layer of the atmosphere, which is different from the ambient temperature at which it can be measured with meteorological instruments and mobile transects.

According to Coltri (2006), the sensors that have the thermal band measure the apparent surface temperature, with a higher value, compared to the air temperature. Thus, "the data from the thermal infrared satellite images are able to provide the qualitative temperature of the city, that is, the design of the local temperature" (2006, p. 101).

Albedo contributes to the identification of surface temperature, being "the ratio of the energy reflected on the incident" (FERREIRA, 2006, p.19), that is, it is the "ability of bodies to reflect the solar radiation that falls on them (MENDONÇA; DANNI-OLIVEIRA, 2006, p.35). It is noteworthy that "the albedo of most of the surface varies with the wavelength and angle of incidence of the light rays" (AYOADE, 2006, p. 27). The different patterns of reflectivity of surface objects occur according

to the color and constitution of the body. In this sense, Saydelles (2005) and Ayoade (2006) point out that lighter and drier objects correspond to higher albedos, in turn, dark and humid objects/bodies absorb more radiation and reflect less.

CORRÊA et al. (2016), state that technological advances in remote sensing have contributed to the improvement of studies of the phenomenon called heat island, due to considerable improvements in the spatial, spectral and temporal resolution of the data. . This means that the sensors operating in this region can have their data converted, after undergoing correction of atmospheric and surface effects (emissivity), into surface temperature (COSTA et al., 2010), considered a parameter of fundamental importance for the study of urban climatology (VOOGT & OKE, 2003).

2.4 REMOTE SENSING

It is remarkable how the importance of satellites has been increasing day by day. News about what is happening in the world, telephone calls, the internet and images used in weather forecasting and monitoring of terrestrial environments are some examples of the benefits that can be obtained using a satellite (FLORENZANO, 2008).

In turn, the term Remote Sensing is recognized as a technology that allows obtaining data from the Earth's surface, through the capture and recording of energy reflected or emitted from the Earth's surface through the detection and quantitative measurement of the responses of electromagnetic radiation interactions with terrestrial materials (FLORENZANO, 2002; MENESES & ALMEIDA, 2012).

Currently, remote sensing has been widely applied to monitor vegetation covers, focusing mainly on their spatial and/or physiological behavior (ABREU; COUTINHO, 2014).

The great revolution of the SR happened in the early 1970s, with the launch of terrestrial natural resources satellites. It was during this period that the fastest development of satellite launch rockets was seen, which made it possible to put artificial satellites into space for various purposes (MENESES, 2012). One of the most important programs developed is the "Landsat" of NASA (National Aeronautics and Space Administration), which began on July 23, 1972 (PARANHOS-FILHO, 2008).

Thus, the evolution of RS is the result of a multidisciplinary effort that involved and involves advances in physics, physical chemistry, chemistry, biosciences and geosciences, computing, mechanics, among other sciences (FIGUEIREDO, 2005).

According to Paranhos-Filho (2008), all types of land cover, such as rocky outcrops, cultivars, forests, and water bodies, absorb a specific portion of the Electromagnetic Spectrum, resulting in a distinct "signature" of electromagnetic radiation. According to the same author, some types of ground cover have a particular spectral response, which distinguishes it from other types of cover, which is why the term "spectral signature" is used (Fig. 2).

Figure 2: Electromagnetic Spectrum Range

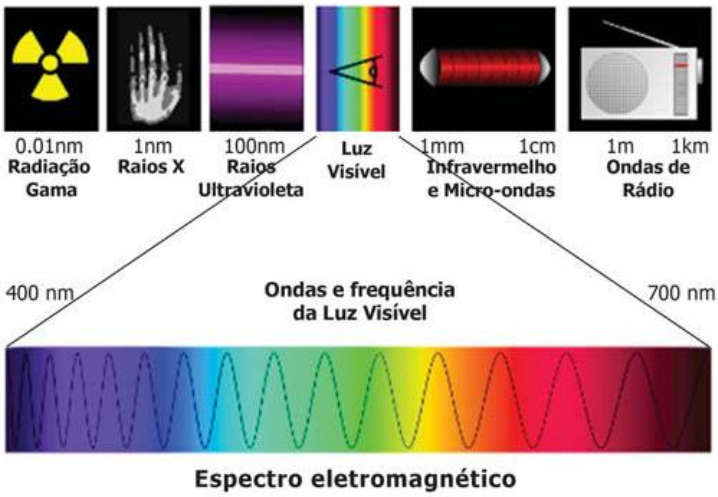

Source: (CONCEIÇÃO e COSTA, 2011)

The Landsat 8 satellite is the latest in its series. Launched on February 11, 2013 by NASA from Vandenberg Air Force Base in California, it operates at an altitude of 705 km, in a heliosynchronous orbit with an inclination of 98.2° (slightly retrograde), similar to the orbits of the Landsat 5 and 7 series. It crosses at the equator at 10:00 (USGS, 2016).

The coverage of the Landsat 8 satellite images occurs practically all over the globe, except for the highest polar latitudes, its temporal resolution is 16 days, the size of the captured scene is approximately 170 km north-south by 183 km east-west.

According to USGS (2016), the platform operates with two imaging instruments, *Operational Land Imager (*OLI) and *Thermal Infrared Sensor* (TIRS). The OLI instrument has 9 spectral bands (1 to 7 and 9), spatial resolution of 30 m, including band 8, panchromatic, with spatial resolution of 15 m. The other imaging system is TIRS, with two pixel bands of 100 m, after processing they are made available with a spatial resolution of 30 meters (Table 1).

Table 1: Landsat 8 Satellite Spatial Information

Bands	Wavelength (Micrometers)	Resolution (Meters)
Band 1 - Coastal Aerosol	0.43 - 0.45	30
Band 2 - Visible Blue	0.45 - 0.51	30
Band 3 - Visible Green	0.53 - 0.59	30
Band 4 - Visible Red	0.64 - 0.67	30
Band 5 - Near Infrared (NIR)	0.85 - 0.88	30
Band 6 - Mid Infrared/SWIR 1	1.57 - 1.65	30
Band 7 - Mid Infrared/SWIR 2	2.11 - 2.29	30
Band 8 - Panchromatic (PAN)	0.50 - 0.68	15
Band 9 - Cirrus	1.36 - 1.38	30

Band 10 - Thermal Infrared (TIRS) 1	10.60 - 11.19	100 (30)
Band 11 - Thermal Infrared (TIRS) 2	11.50 - 12.51	100 (30)

2.5 GEOGRAPHIC INFORMATION SYSTEMS (GIS)

The use of GIS and remote sensing techniques in different areas of the earth's surface has achieved satisfactory, consistent and important results for the monitoring and management of natural resources, especially in urban areas (SOUZA et al., 2016).

Geographic Information Systems (GIS) are fundamental tools for the application of digital image processing techniques, they have several algorithms, among them the Thermal, capable of transforming thermal infrared data into apparent surface temperature, essential for the interpretation of these data (MASHIKI, 2012).

From the thermal band, it is possible to obtain values relative to the surface temperature, thus identifying areas with ICU, especially in urban areas.

SANTANA et al. (2014) state that the use of remote sensing images and geographic information system techniques are important instruments for the evaluation of environmental changes, especially in the relationship between land use and occupation in the thermal field in urban areas, as they allow the understanding of the dynamics of biophysical processes and the interaction between soil, plant and atmosphere in urban areas.

2.6 LAND USE AND OCCUPATION IN THE URBAN AREA

The constant presence of solar radiation acting on the urban layer causes greater thermal differentiation between areas with many buildings and areas with fewer buildings and less soil sealing (ROCHA et al., 2011).

According to ASEADA et al. (1996), the time range where the asphalt pavement exhibits a greater heat flow is from 9:00 a.m. to 12:00 p.m.

The high irradiation emitted into the atmosphere drastically interferes with the local energy balance, causing an immediate reflection on temperature (SERRATO et al., 2002).

According to ALVES & VECCHIA (2012), some surfaces take longer to lose the absorbed energy, and are able to maintain a high energy flow for longer during the day, such as asphalt.

The morphology of heat islands is, for the most part, always the same: cement, cement and asbestos tiles and asphalt. The intensity of heat islands is closely related to the amount of green area, so all ICU's are characterized by an excess of civil construction material and little or no green area (COLTRI et al., 2007), as shown in Figure 1

The exposed soil, without vegetation cover, has a high thermal amplitude, heating up rapidly during the period of sun exposure, leading to a consequent rise in temperature during the day, increasing heat irradiation and the temperature in its surroundings (MASHIKI, 2012).

According to GARTLAND (2010), the presence of vegetation reduces the effects of heat islands in two ways: through the shade provided by the tree canopy and also due to the process of evapotranspiration, which increases the relative humidity of the air and decreases the relative temperature of the air.

Environmental characterization can be carried out using bioindicator species, in view of the prior knowledge of the ecological characteristics and behavior of communities in natural and adverse situations (PIMENTA et al., 2016).

2.7 SURFACE TEMPERATURE IN URBAN AND PERI-URBAN AREA

Surface temperature is one of the main data that can be estimated from thermal band images. The Earth's surface temperature has been the subject of several studies (ADAMI et al., 2008; SILVA et al., 2011; FORMIGONI et al., 2011) and widely applied in meteorology and natural resources analysis, especially in the structuring of energy balance models, biophysical and bioclimatic parameters of the surface.

For these studies, the use of remote sensing images and geographic information system techniques are important instruments for the evaluation of environmental changes, especially in the relationship between land use and occupation in the thermal field in urban areas, as they allow the understanding of the dynamics of biophysical processes and the interaction between soil, soil and soil plant and atmosphere in urban areas (SANTANA et al., 2014). The use of GIS and remote sensing techniques in different areas of the earth's surface has achieved satisfactory, consistent and important results for the monitoring and management of natural resources, especially in urban areas.

Surface temperature refers to the heat flux given as a function of the energy that arrives and leaves the body, and is of paramount importance for understanding the interactions between the Earth's surface and the atmosphere. The best range that allows for greater transmission of the energy emitted from Earth that reaches the sensor in the thermal infrared region of the electromagnetic spectrum is the range of 8.0 to 14.0 um (STEINKE et al, 2010).

According to MARALET et al. (1985), surface temperature is obtained by converting the digital number (DN) of each pixel of the thermal canal image into apparent surface temperature.

MASHIKI (2012) states that several studies have used the surface temperature estimation obtained through remote sensing, however, he highlights the placement of JARDIM (2007), where he addresses important aspects about heat islands:

> [...] The "heat island" does not represent the reality of the urban climate, but one of its aspects, translated by a momentary or hourly situation, motivated by the punctual convergence of factors linked to the characteristics of relief conformation, arrangement of equipment and urban dynamics, under the influence of certain types of weather, associated with atmospheric systems at a given stage of their temporal evolution.

2.8 URBAN VEGETATION

Tree canopies play an important role in the attenuation of radiation and consequently the reduction of the thermal amplitude in adjacent areas (RIBEIRO et al., 2015).

According to PENG et al. (2012) the absence of vegetation alters the participation of energy flows on the surface, reducing the latent heat flux, consequently increasing the sensible heat flux. This statement corroborates MASHIKI (2012), where he states that any type of vegetation has an influence on the mitigation of heat islands.

GARTLAND (2010) states that vegetation absorbs water through its roots and emits steam through its leaves, a process called evapotranspiration, where it removes heat from the air to evaporate water, which can reduce air temperature peaks during the summer.

According to ABREU (2008), plant evapotranspiration has a beneficial effect on the climate of urban areas, where it absorbs calories, reducing the temperature of the local microclimate in times of greater heat wave.

A roof can lower the air temperature by 2ºC, while the shade of a sweating tree can reduce the temperature by 4ºC (PRIMAVESI et al, 2007).

The presence of vegetation masses can promote the opposite effect to the heat island phenomenon, and favor the occurrence of islands of freshness, where FERREIRA et al (2015) studying islands of freshness, state that green areas promoting islands of freshness, contribute to minimize the extreme effects of solar radiation, temperature and relative humidity of the air, improving the environmental conditions of urbanized spaces.

For NINCE et al. (2014), the direct effects of shading by vegetation can be quantified by measuring the surface temperature of materials exposed to and protected by tree canopies. A shaded area is weakly affected by the incident direct solar radiation, and thus the radiant temperature of that surface is lower, which decreases the longwave radiation emitted.

The vegetation cover can absorb up to 50% of shortwave radiation and up to 95% of longwave radiation (BARBIRATO et al, 2007). Short-wave radiation is that which comes from solar radiation and long-wave radiation that emits from the Earth's surface.

According to Oliveira (2011), one of the solutions to alleviate the problems caused by urbanization is to treat the urban environment with vegetation, through the afforestation of public roads and the creation of protected natural areas. However, areas with no vegetation, or the same with a high level of degradation, have characteristics of emissivity like exposed soil, as stated by ALVES & VECCHIA (2012), corroborating GARTLAND (2010), where exposed soil without vegetation cover has a high thermal amplitude, heating up rapidly during the period of sun exposure, increasing heat irradiation and temperature in its surroundings.

3 MATERIALS AND METHODS

3.1 AREA OF STUDY

The municipality of Ilha Solteira is in the northwest of the State of São Paulo, in the most strategic position of the Tietê-Paraná Waterway, with a total area of 661.3 km². Of this total, 5.82 km² make up the urban area (MIRANDA et al., 2005; SILVA et al., 2006). According to the Köeppen International System, the climate of this region is humid tropical, with a rainy season in the summer and a dry season in the winter (Aw). Average monthly temperatures range from 21.5 °C (July) to 26.4 °C (December), and average monthly rainfall ranges from 20 mm (July) to 225 mm (January). The period of water surplus extends from January to February, and the period of water deficit, from March to December. The average wind speed is classified as weak, and its predominant direction is E-SE (HERNANDEZ, 2007). The relief of the study area is hilly, with a predominance of wide and medium hills (SÃO PAULO, 1981). More than 80% of the urban area has slopes ranging from 0 to 5%, and the predominant slope orientation classes are south-west (SW) and west (W) (SANTOS, 2005). The soil present in the study area is of the dytrophic A Red Latosol type, with a clayey texture, flat relief and smooth undulating (LV39) (EMBRAPA, 1999). In Ilha Solteira, there are green areas called Leisure Area, located in the northern position of the urban perimeter, with 11.35 ha, occupied with the species *Pinus elliottii* and Zoo, located in the western position of the urban perimeter, with 18 ha, occupied with predominant vegetation of the Atlantic Forest biome (Semi-Deciduous Dry Forest) (COSTA et al., 2010). Figure 3 corresponds to the location of the municipality of Ilha Solteira in the state of São Paulo and the limit of the urban area within the municipality. And Figure 4 shows the borders with other municipalities.

Figure 3: Location Map of the Municipality and City of Ilha Solteira

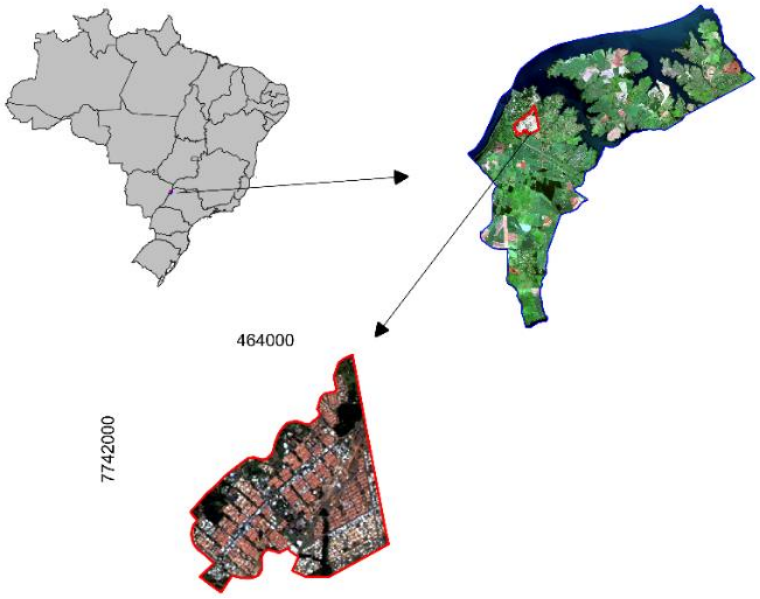

Source: Prepared by the author.

Figure 4: Boundary of Ilha Solteira and its borders:

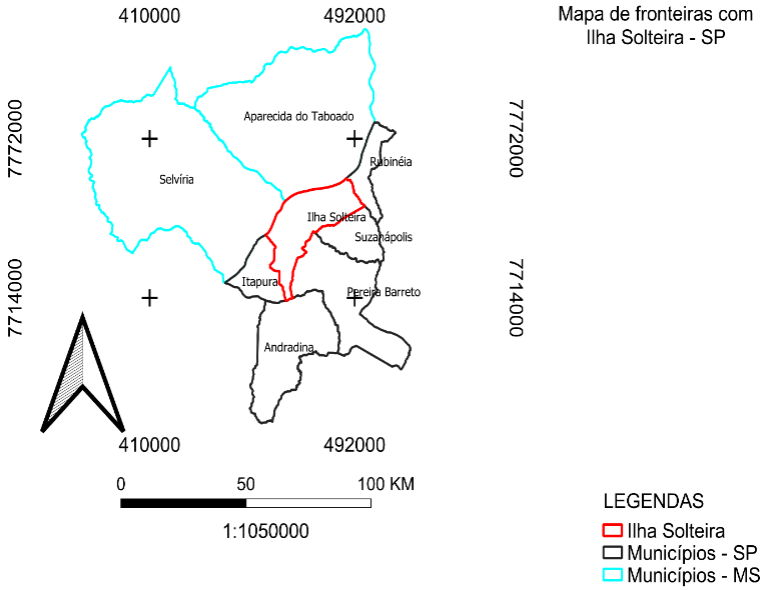

Source: Prepared by the author.

3.2 IMAGE ACQUISITION

For the execution of this work, a survey of free orbital images was carried out, available in the United States Geological Survey (USGS), (www.usgs.gov), through the Landsat 8 satellite, TIRS (Thermal Infrared Sensor). Cloudcover-free images were chosen (Tables 2, 3, 4 and 5).

Table 2: Images taken from the Landsat 8 satellite from the year 2018

2018	Image Date	Orbit/Point	Seasons
1	19/08/2018	222/074	Winter (1)
2	11/09/2018	223/074	Winter (2)
3	29/04/2018	222/074	Autumn (1)
4	31/05/2018	222/074	Autumn (2)
5	22/10/2018	222/074	Spring (1)
6	16/12/2018	223/074	Spring (2)
7	11/02/2019	222/074	Summer (1)

Table 3: Images obtained from the Landsat 8 satellite in 2019

2019	Image Date	Orbit/Point	Season of the Year
1	28/07/2019	223/74	Winter (1)
2	07/09/2019	222/74	Winter (2)
3	31/03/2018	222/074	Autumn (1)
4	10/06/2018	223/074	Autumn (2)
5	25/10/2019	222/074	Spring (1)
6	17/11/2019	223/074	Spring (2)
7	14/02/2020	222/074	Summer (1)
8	13/03/2019	222/074	Summer (2)

Table 4: Images obtained from the Landsat 8 satellite in 2020

2020	Image Date	Orbit/Point	Season of the Year
1	08/08/2020	222/074	Winter (1)
2	16/09/2020	223/074	Winter (2)
3	21/06/2020	222/074	Autumn (1)
4	20/05/2020	222/074	Autumn (2)
5	11/10/2020	222/074	Spring (1)
6	28/11/2020	222/074	Spring (2)
7	07/02/2021	223/074	Summer (1)
8	23/02/2021	223/074	Summer (2)

Table 5: Images obtained from the Landsat 8 satellite in 2021

2021	Image Date	Orbit/Point	Season of the Year
1	11/08/2021	222/074	Winter (1)
2	12/09/2018	222/074	Winter (2)
3	21/04/2021	222/074	Autumn (1)
4	15/06/2021	223/074	Autumn (2)
5	06/11/2021	223/074	Spring (1)
6	08/12/2021	223/074	Spring (2)
7	10/02/2022	223/074	Summer (1)
8	07/03/2022	222/074	Summer (2)

3.3 IMAGE FUSION

The image fusion technique was performed for the images of all dates, obtained from the Landsat 8 satellite, with the objective of integrating the band with the best spatial resolution, band 8, panchromatic (spatial resolution of 15m), with the bands with the lowest resolution, band 2 to 7 (spatial resolution of 30m). For image fusion, the IHS method is one of the most widely used, due to its efficiency and ease of implementation (TU et al., 2001).

As it is a small urban area, the integration of the panchromatic band with those with lower spatial resolution is essential, as it brings together both characteristics in a new image, making it possible to obtain a better visualization and interpretation of the study area (Figure 5). The GIS QGis 3.16 Hannover was used to generate the fused images

Figure 5: Raw Image (A) and Fused Image (B)

A) Imagem LandSat com resolução espacia de 30M

B) Imagem LandSat com resolução espacial de 15M

Source: Prepared by the author.

3.4 BEAUFORT SCALE

The Beaufort Scale aims to measure the intensity of the winds through observations, since the scale itself was constructed in this way. Created by Sir Francis Beaufort, this scale was widely used by the British Royal Navy. In this study, the Beaufort Scale (Figure 6) was used as a parameter to classify the magnitude of the winds as: Weak (0 -3), Moderate (4 – 6) and Strong (>7).

Figure 6: Beaufort scale modified by the Department of Protection and Civil Defense of the Municipality of Santo André

Grau	Designação	m/s	km/h	Efeitos em terra
0	*Calmo*	<0,3	<1	Fumaça sobe na vertical
1	*Aragem*	0,3 a 1,5	1 a 5	Fumaça indica direção do vento
2	*Brisa leve*	1,6 a 3,3	6 a 11	As folhas das árvores movem; os moinhos começam a trabalhar
3	*Brisa fraca*	3,4 a 5,4	12 a 19	As folhas agitam-se e as bandeiras desfraldam ao vento
4	*Brisa moderada*	5,5 a 7,9	20 a 28	Poeira e pequenos papéis levantados; movem-se os galhos das árvores
5	*Brisa forte*	8 a 10,7	29 a 38	Movimentação de grandes galhos e árvores pequenas
6	*Vento fresco*	10,8 a 13,8	39 a 49	Movem-se os ramos das árvores; dificuldade em manter um guarda chuva aberto; assobio em fios de postes
7	*Vento forte*	13,9 a 17,1	50 a 61	Movem-se as árvores grandes; dificuldade em andar contra o vento
8	*Ventania*	17,2 a 20,7	62 a 74	Quebram-se galhos de árvores; dificuldade em andar contra o vento; barcos permanecem nos portos
9	*Ventania forte*	20,8 a 24,4	75 a 88	Danos em árvores e pequenas construções; impossível andar contra o vento
10	*Tempestade*	24,5 a 28,4	89 a 102	Árvores arrancadas; danos estruturais em construções
11	*Tempestade violenta*	28,5 a 32,6	103 a 117	Estragos generalizados em construções
12	*Furacão*	>32,7	>118	Estragos graves e generalizados em construções

Source: https://www3.santoandre.sp.gov.br/defesacivil/escala-de-beaufort/

3.5 SURFACE TEMPERATURE

Using the QGIS GIS, the surface temperature image (Ace) was generated, where the band 10 (thermal) of the Landsat-8 satellite, TIRS sensor, which has a spatial resolution of 30 meters, was used. To generate the temperature image, the crawl calculator tool was used, a tool implemented in the GIS, inserting Equation 1, proposed by the USGS (2015) where, based on the metadata contained in the image set, the conversion of gray levels to radiance was performed:

$$L\lambda = ML * Qcal + AL \quad (1)$$

Where:

Lλ = Spectral Radiance at the top of the atmosphere in Watts/ (m²*sr*µm)

ML = Band 10 Resizing Multiplicative Factor (3.3420E-04)

Qcal = Quantized value calibrated by the pixel in DN (band 10)

LA = Band 10 Specific Additive Resize Factor (0.10000)

After the radiance image was generated, this result was converted to surface temperature (Ts) image, but the image resulting from this conversion presents its data

In Kelvin temperature, according to Coelho and Correa (2013), there is a need to implement Equation 2, proposed by USGS (2015), subtracting 273.15 from its result, to obtain an image of temperature in degrees Celsius, as follows:

$$Ts = K2 \ln (K1 L\lambda + 1) - 273.15 \quad (2)$$

Where:

Ts = Surface temperature, in degree Celsius (ºC)

K1 = Calibration constant 1 (774.89)

K2 = Calibration constant 2 (1.321.08)

Lλ = Spectral radiance in Watts/ (m²*sr*µm)

However, the simplified formula was used by joining Equations 1 and 2, the result is below:

TC= (1321.08/Ln (774.89/ (3.3420E-04* "banda10.tif" + 0.10000) +1)) -273.15

3.6 IDENTIFICATION OF AREAS WITH URBAN HEAT ISLANDS (ICU'S)

A georeferenced database was created for the analysis, exploration and display of spatial information processed using QGis 3.16 Hannover.

After importing the processed images containing the surface temperature, and the high spatial resolution image, Landsat, we continued with the import of vector data: limits of the urban area. Based

on the limit of the urban area, a buffer (200m) was created, covering the rural area surrounding the urban perimeter, which is the reference area for analyzing the occurrence of ICU within the city of Ilha Solteira, as shown in (Figure 7).

Figure 7: Delimitation of the urban area and surrounding área

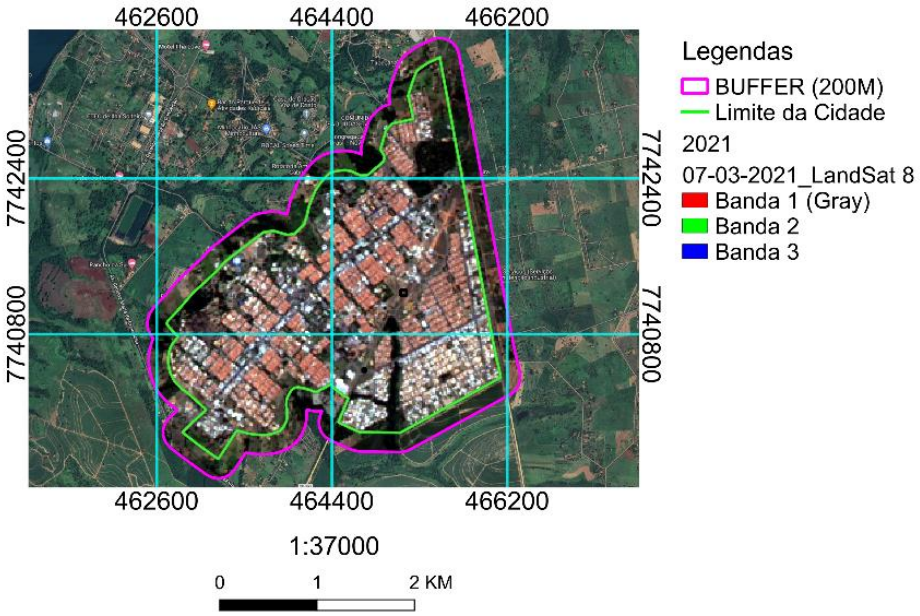

Source: Prepared by the author.

4 RESULTS

2018

4.1 WINTER 1

4.1.1 Urban Heat Island on 19/08/2018

In the surface temperature image, obtained on 08/19/2018, corresponding to the winter season (Figure 8), the occurrence of areas with UCI was not found.

Figure 7: Map of Urban Heat Islands in Ilha Solteira – SP, on 08/19/2018

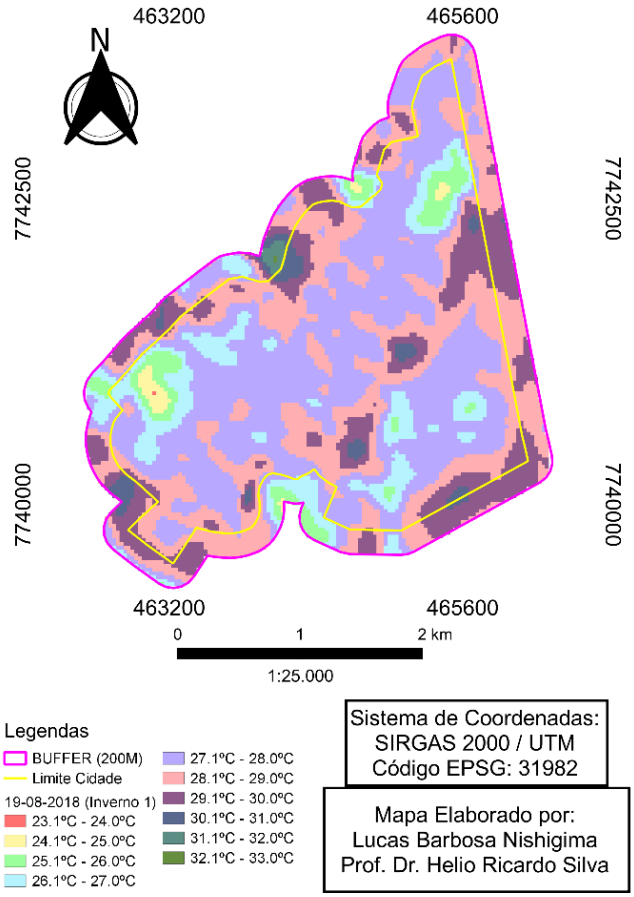

Source: Prepared by the author.

4.2 WINTER 2

4.2.1 Urban Heat Island on 11/09/2018

In the surface temperature image, obtained on 09/11/2018, corresponding to the winter season (Figure 9), the occurrence of areas with UCI was not found.

Figure 8: Map of Urban Heat Islands in Ilha Solteira – SP, on 09/11/2018

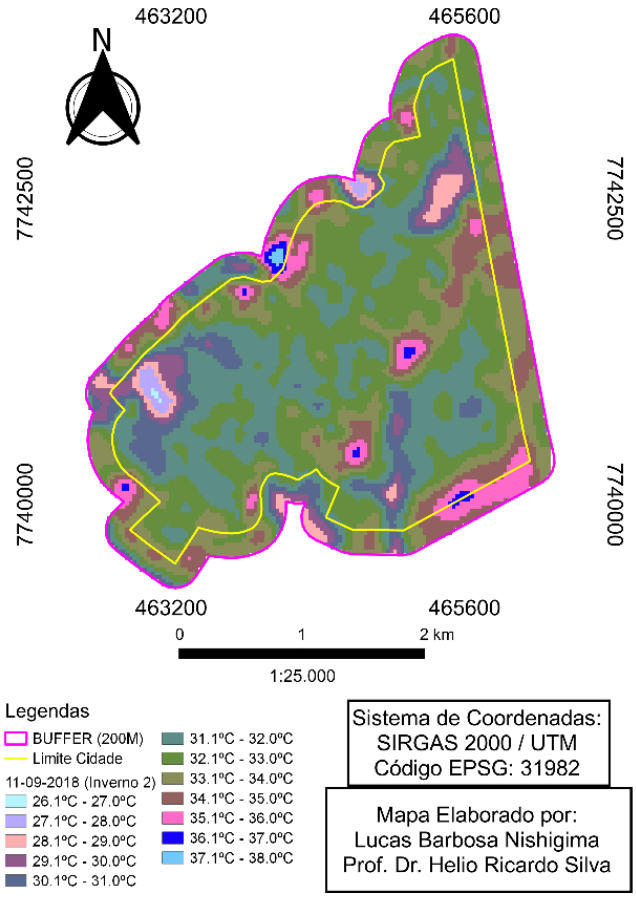

Source: Prepared by the author.

4.3 FALL 1

4.3.1 Urban Heat Island on 29/04/2018

In the surface temperature image, obtained on 04/29/2018, corresponding to the winter season (Figure 10), the occurrence of areas with ICU was not found.

Figure 9: Map of Urban Heat Islands in Ilha Solteira – SP, on 04/29/2018

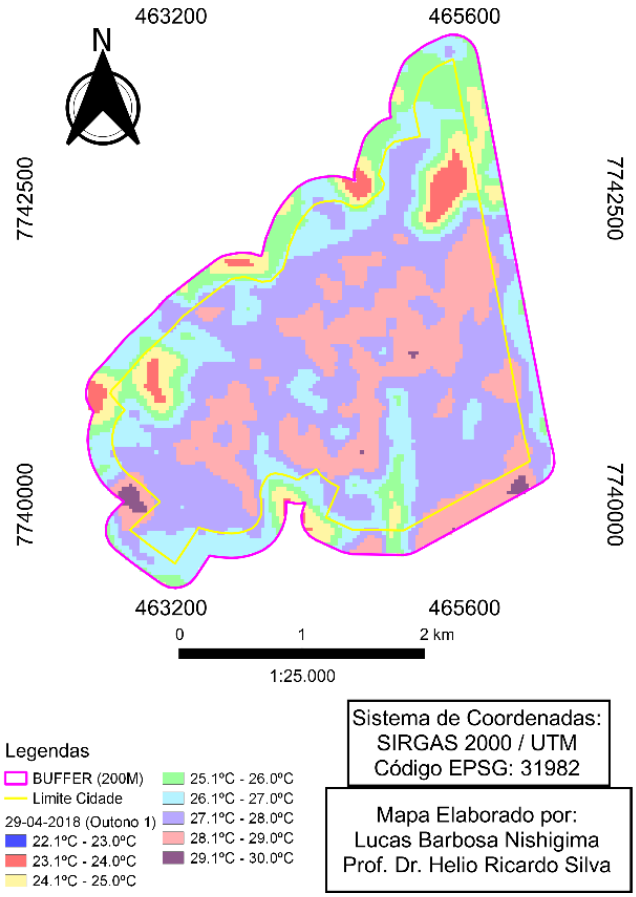

Source: Prepared by the author.

4.4 FALL 2

4.4.1 Urban Heat Island on 31/05/2018

According to the data obtained on 05/31/2018 (Figure 11), 1 area with heat islands within the urban perimeter was identified, called Area 1. The area within the limit of 200m (surroundings) used as a reference for the identification of ICUs was under the temperature of 26.1 to 27°C.

Location: Gerson Dourado de Oliveira Highway

Reference: Correrilha - Physical Exercise Advisory

Figure 10: Map of Urban Heat Islands in Ilha Solteira – SP, on 05/31/2018

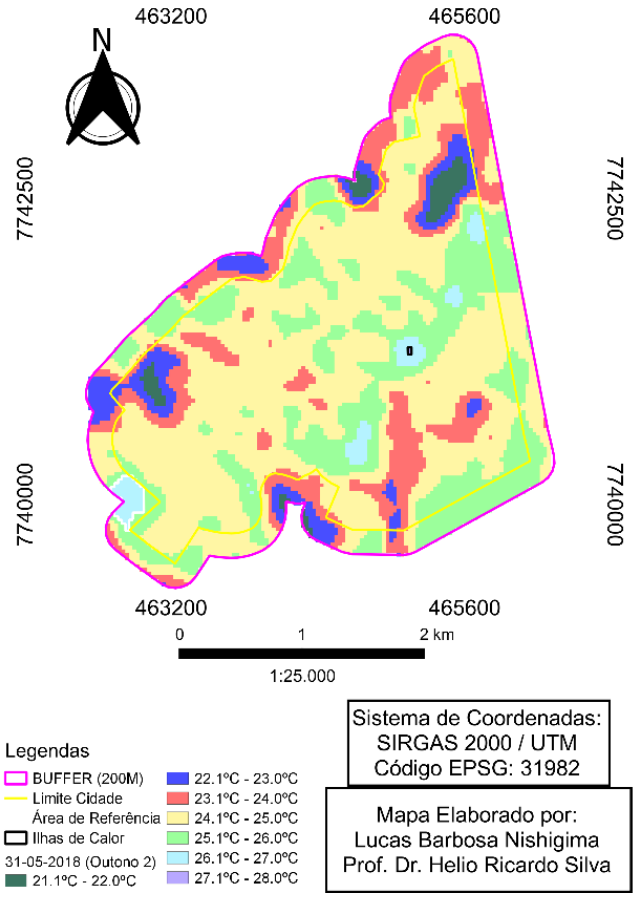

Source: Prepared by the author.

Table 3: ICU area measurements as of 05/31/2018

	Fall (2)		
	Heat Islands		
27.1ºC - 28.0ºC	Urban Boundary	Areas ICU	TOTAL
Area (ha)	734,913	0,181	735,094
Area (%)	99,976	0,024	100

Figure 11: Map of Urban Heat Islands in Ilha Solteira – SP, on 05/31/2018

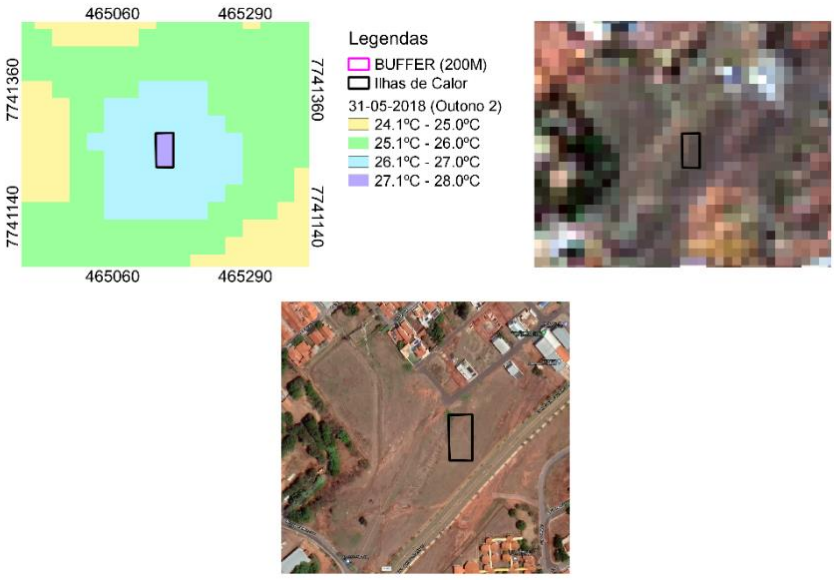

Source: Prepared by the author.

4.5 SPRING 1

4.5.1 Urban Heat Island on 22/10/2018

According to the data obtained on 10/22/2018 (Figure 13), 3 areas with heat islands were identified within the urban perimeter, called Areas 1, 2 and 3. The area within the limit of 200m (surroundings) used as a reference for the identification of the ICU was under the temperature of 31.1 to 32°C.

Location: R. Olinda and R. Floresta (Natural Well-Being), Pas. Caruaru (Thai Accessory and Silva) and Pas. Juazeiro (CrTatto Studio) (North Region)

Figure 12: Map of Urban Heat Islands in Ilha Solteira – SP, on 10/22/2018

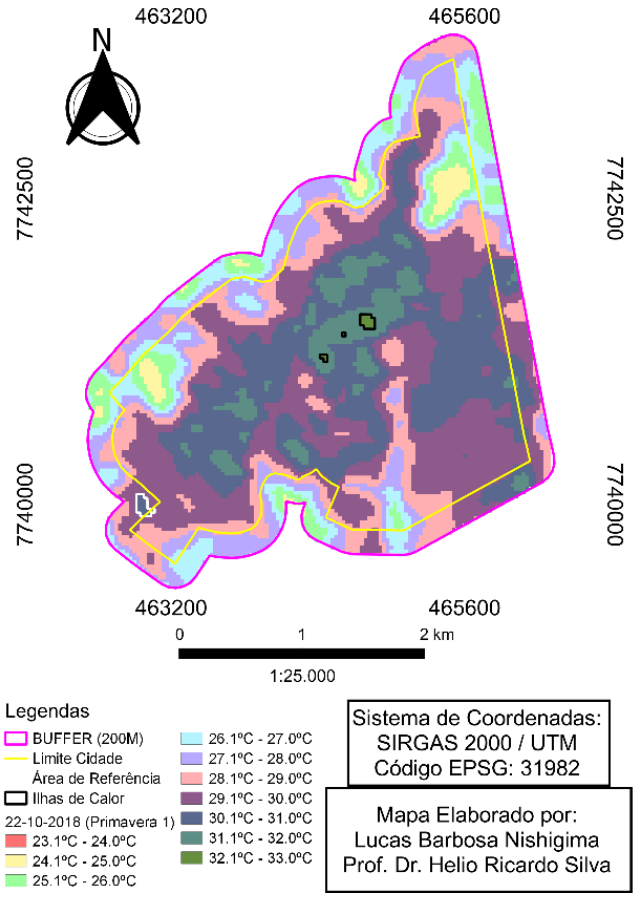

Source: Prepared by the author.

Table 4: ICU area measurements as of 10/22/2018

	Spring (1)		
	Heat Islands		
32.1ºC - 33.0ºC	Urban Boundary	Area ICU	TOTAL
Area (ha)	734,913	1,615	736,528
Area (%)	99,78	0,22	100

Figure 13: Map of Urban Heat Islands in Ilha Solteira – SP, on 10/22/2018

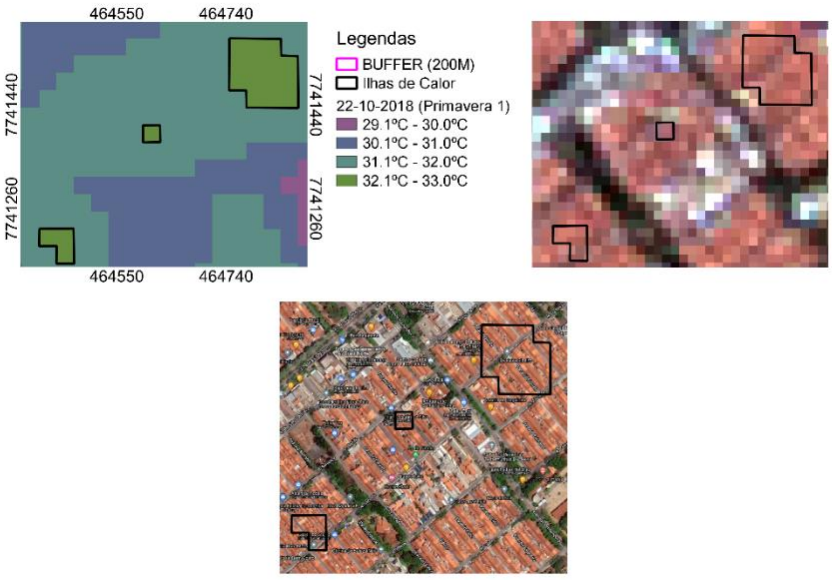

Source: Prepared by the author.

4.6 SPRING 2

4.6.1 Urban Heat Island on 12/16/2018

According to data obtained on 12/16/2018 (Figure 15), 19 areas with heat islands were identified within the urban perimeter, called Areas 1, 2, 3, 4, 5, 6, 7, 8, 9, 10, 11, 12, 13, 14, 15, 16, 17, 18 and 19. The area within the limit of 200m (surroundings) used as a reference for the identification of the ICU was under the temperature of 31.1 to 32°C.

Local: 32.1 até 33.0ºC: R. Londrina, R. Curitiba, Av. Brasil Sul, Al. Santa Catarina, Pas. Laguna, Pas. Itu, Al. Paraná, R. Maringá, R. Ivaí, R. Uberaba, R. Belo Horizonte, R. Rio Paraíba, R. Cuiabá, R. Corumbá, R. Goiânia, Pas. Recife, R. Caracol, Pas. Batalha, R. Imperatriz, R. Rio Tocantins, R. Rio Carnaíba, R. São Luís, R. Icaraí, R. Manaus, R. Canindé, Pas. Oros, R. Sete de Setembro, R. 25, R. 23, R. 29, R. 31, Av. 15 de Outubro, Pas. Araras, R. Limeira, R. 9, Al. Bahia, R. Laguna, R. Sorocaba, Pas. Araras, R. Limeira, Pas. Salvador, Pas. Juazeiro, Pas. Recife, Pas. Floresta, Pas. Olinda, R. Fortaleza, Pas. Sobral, Pas. Imperatriz, Al. Bahia, Pas. Cabo, R. Recife, Pas. Caruaru, R. Olinda, R. Floresta, Pas. Sobral, R. Fortaleza, R. Salvador, R. Rio Iguaçu, Pas. Santos.

Figure 14: Map of Urban Heat Islands in Ilha Solteira – SP, on 12/16/2018

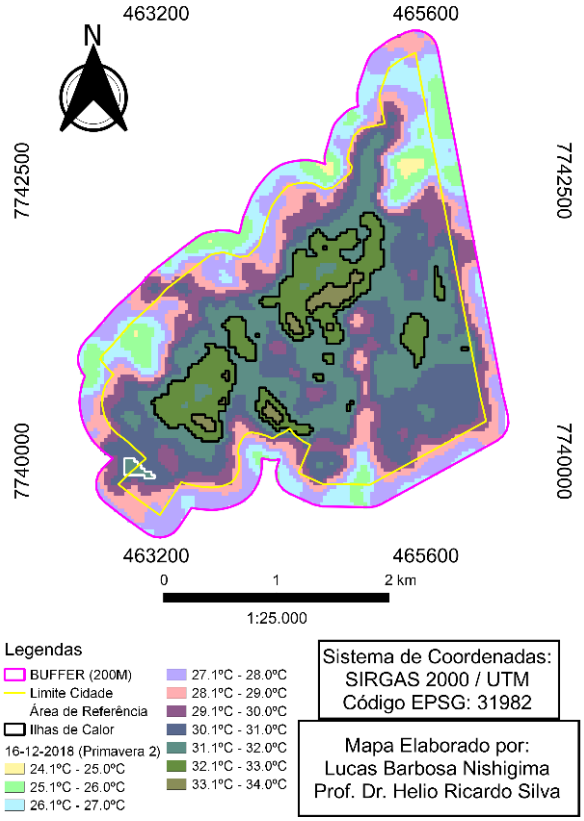

Source: Prepared by the author.

Table 5: ICU area measurements as of 12/16/2018

	Spring (2)		
	Heat Islands		
32.1ºC - 34.0ºC	Urban Boundary	Areas ICU	TOTAL
Area (ha)	734,913	138	872,913
Area (%)	81,22	18,78	100

Figure 15: Map of Urban Heat Islands in Ilha Solteira – SP, on 12/16/2018

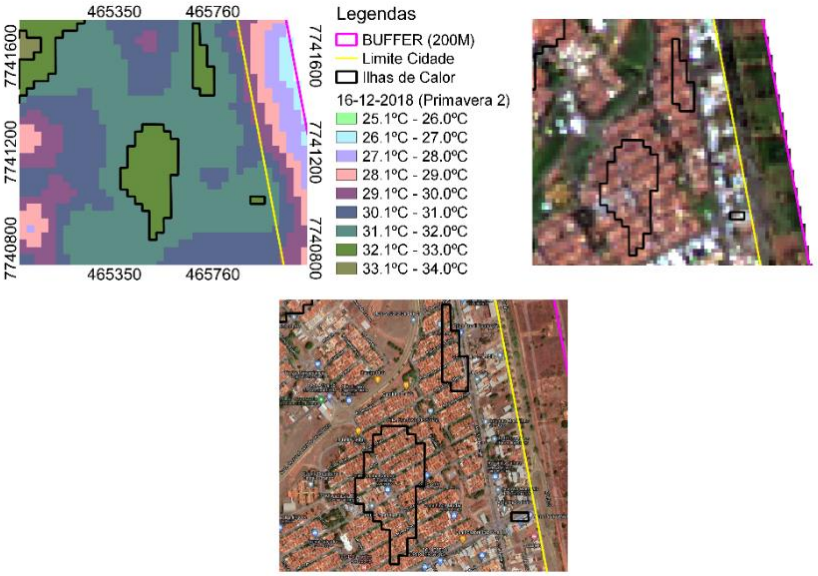

Source: Prepared by the author.

Figure 16: Map of Urban Heat Islands in Ilha Solteira – SP, on 12/16/2018

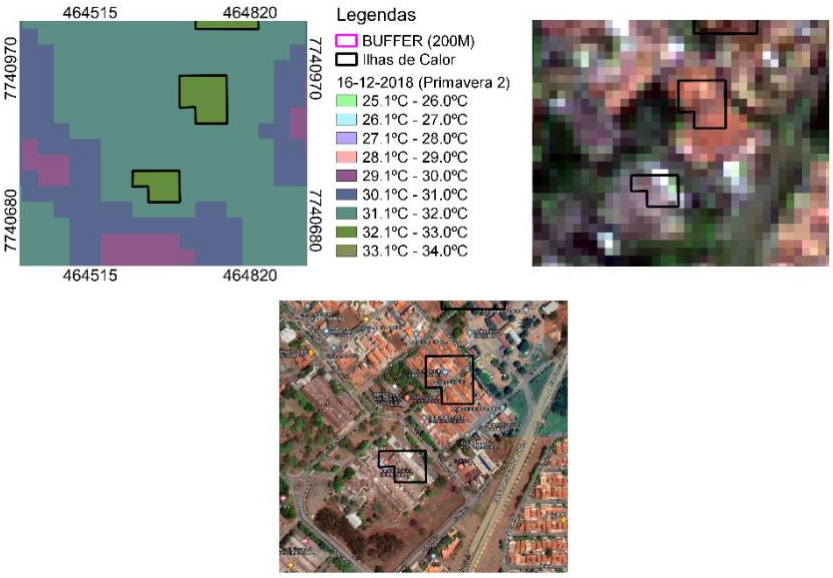

Source: Prepared by the author.

Figure 1817Map of Urban Heat Islands in Ilha Solteira – SP, on 12/16/2018

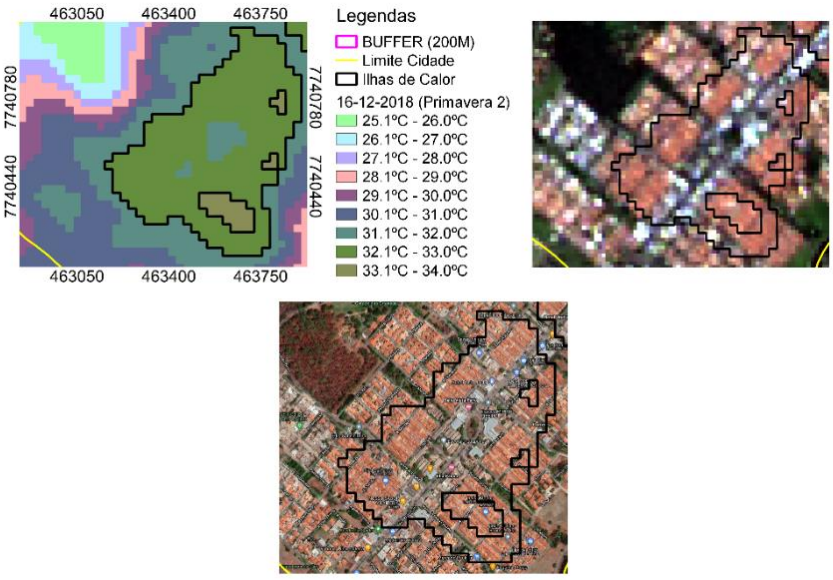

Source: Prepared by the author.

Figure 18: Map of Urban Heat Islands in Ilha Solteira – SP, on 12/16/2018

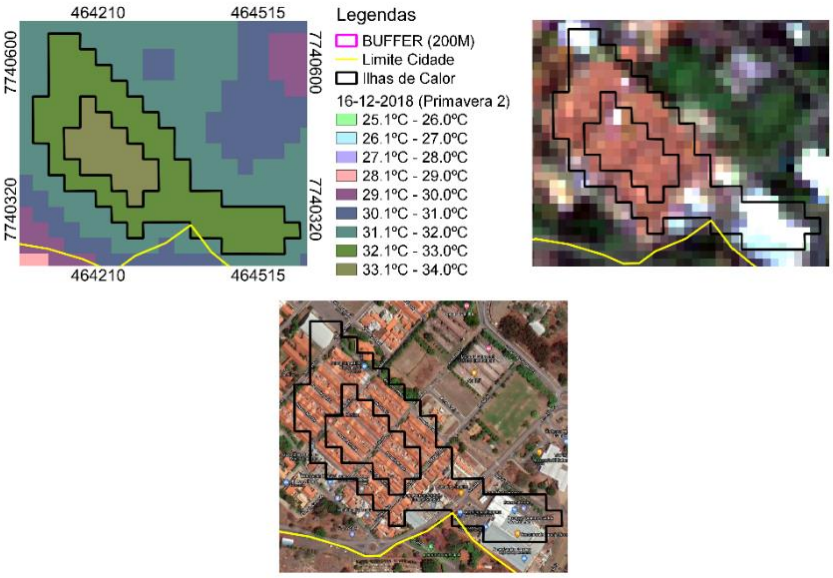

Source: Prepared by the author.

Figura 19: Mapa de Ilhas de Calor Urbana em Ilha Solteira – SP, em 16/12/2018

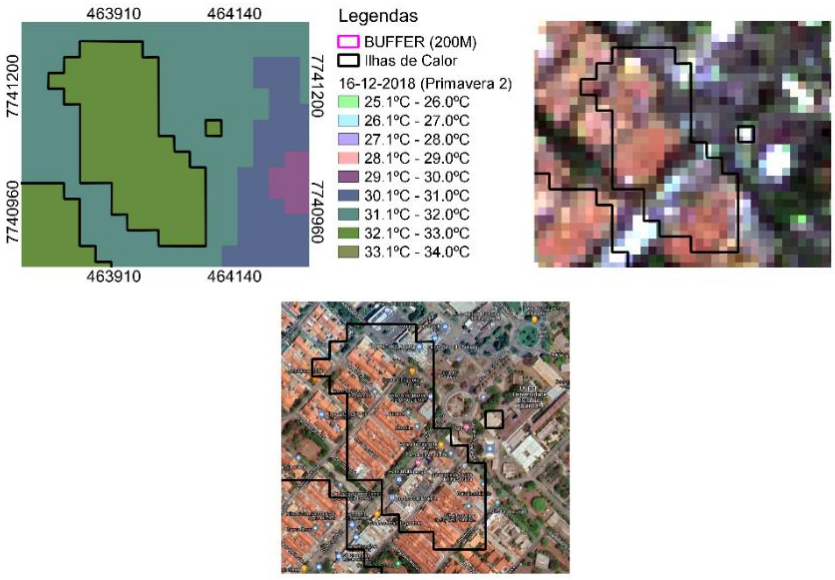

Source: Prepared by the author.

Figure 20: Map of Urban Heat Islands in Ilha Solteira – SP, on 12/16/2018

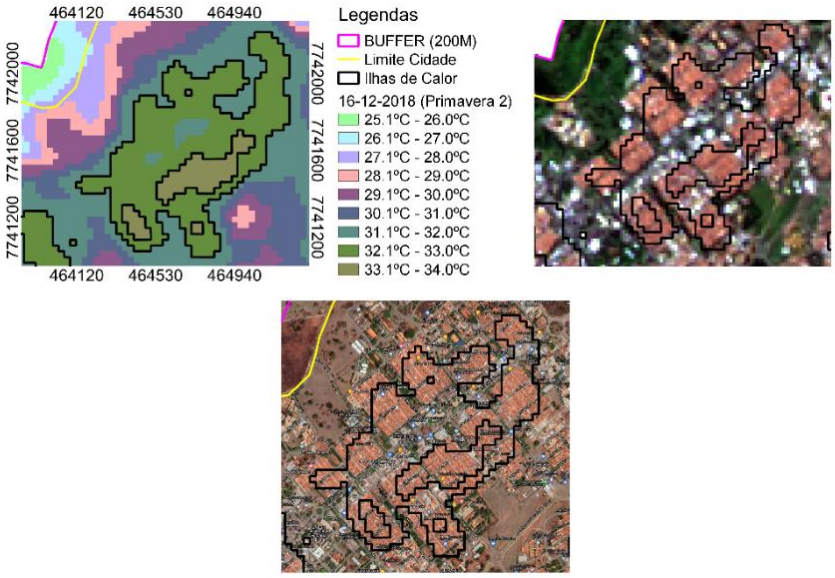

Source: Prepared by the author.

4.7 SUMMER 1

4.7.1 Urban Heat Island on 22/02/2019

According to the data obtained on 02/22/2019 (Figure 22), 1 area with heat islands was identified within the urban perimeter, called Area 1. The area within the limit of 200m (surroundings) used as a reference for the identification of the ICU was under the temperature of 24.1 to 25°C.

The area called Area 1 had a temperature of 25.1 to 26°C, 1°C above the reference area.

Location: R. Olinda.

Figure 2221Map of Urban Heat Islands in Ilha Solteira – SP, on 02/22/2019

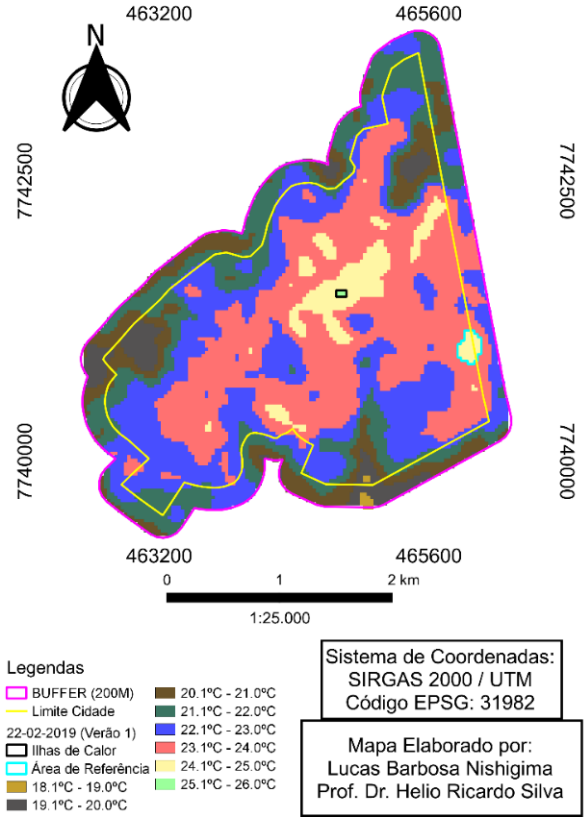

Source: Prepared by the author.

Table 6: ICU area measurements as of 02/22/2019

	Summer (1)		
	Heat Islands		
32.1ºC - 34.0ºC	Urban Boundary	Areas ICU	TOTAL
Area (ha)	734,913	0,539	735,452
Area (%)	99,93	0,07	100

Figure 22: Map of Urban Heat Islands in Ilha Solteira – SP, on 02/22/2019

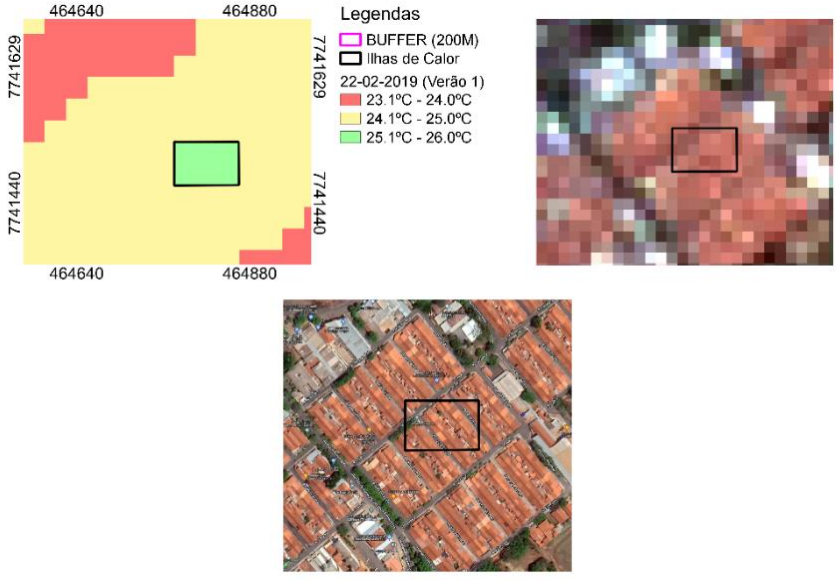

Source: Prepared by the author.

4.8 SUMMER 2

4.8.1 Urban Heat Island on 06/03/2019

According to data obtained on 03/06/2019 (Figure 24), 17 areas with heat islands were identified within the urban perimeter, called Areas 1, 2, 3, 4, 5, 6, 7, 8, 9, 10, 11, 12, 13, 14, 15, 16 and 17. The area within the limit of 200m (surroundings) used as a reference for the identification of the ICU was under the temperature of 29.1 to 30°C.

Local: 30.1ºC a 31ºC: R. Curitiba, Al. Paraná, R. Maringá, R. Rio Ivaí, Pas. Uberaba, R. Uberaba, Al. Minas Gerais, R. Belo Horizonte, Pas. Belo Horizonte, Pas. Caxambu, R. Rio Paraíba, Av. Brasil Sul, Al. São Paulo, Pas. Santos, R. Santos, Pas. Sorocaba, R. Sorocaba, Pas. Bauru, Pas. Laguna, R. Rio Iguaçu, R. Tijucas, Pas. Tijucas, Al. Santa Catarina, Pas. Corumbá, R. Marilia, Pas. Marilia, Pas. Limeira, R. Limeira, Pas. Araras, R. Piracicaba, R. Guanabara, R. Jequié, Pas. Jequié, R. Salgueiro, Pas. Salgueiro, Pas. Cabo, R. Nazaré, R. Ilhéus, Pas. Ilhéus, R. Juazeiro, Pas. Juazeiro, R. Salvador, Pas. Salvador, R. Rio São Francisco, Pas. Recife, R. Recife, Pas. Caruaru, R. Caruaru, Pas. Floresta, R. Floresta, R. Olinda, Pas. Olinda, R. Rio Ipanema, Al. Pernambuco, R. Fortaleza, Pas. Fortaleza, Pas. Sobral, R. Sobral, Al. Ceará, Pas. Canindé, Pas. Icaraí, R. Icaraí, Av. Brasil Norte, Pas. Imperatriz, R. Imperatriz, R. Colinas, Pas. Colinas, Pas. Monção, Al. Maranhão, R., Arati, Pas. São Luís, R. São Luís, R. Manaus, Pas. Manaus, R. Onelio Buttarello, R. Vinte e Quatro,

R. Sete de Setembro, Av. Quinze de outubro, R. Goiânia, Pas. Cristalina, Pas. Goiânia, Pas. Barras, R. Teresina., Pas. Caracol, Pas. Batalha, R. Caracol, R. Batalha, Pas. Correntes, R. Correntes.

31.1ºC to 32ºC: R. Recife, Pas. Floresta

Figure 23: Map of Urban Heat Islands in Ilha Solteira – SP, on 03/06/2019

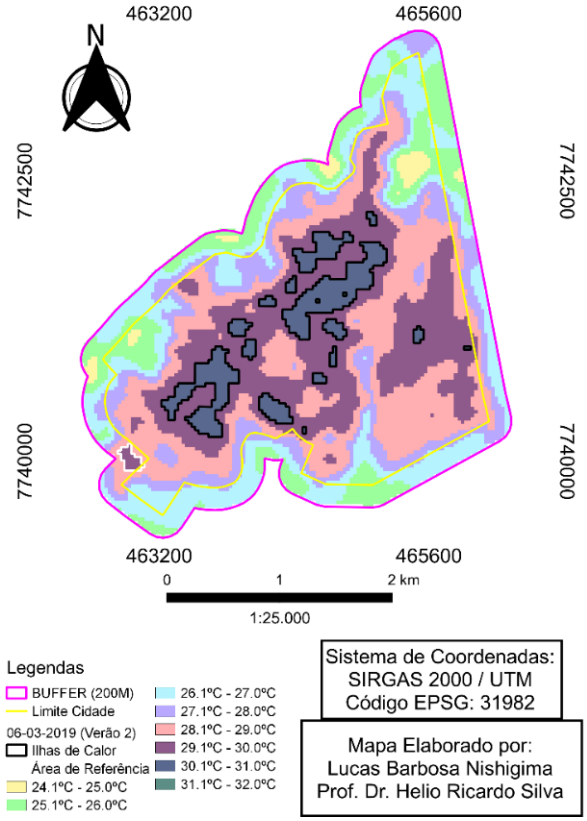

Source: Prepared by the author.

Table 7: ICU area measurements as of 03/06/2019

	Summer (2)		
	Heat Islands		
30.1ºC - 32.0ºC	Urban Boundary	Areas ICU	TOTAL
Area (ha)	734,913	74,339	809,252
Area (%)	89,88	10,12	100

Figure 24: Map of Urban Heat Islands in Ilha Solteira – SP, on 03/06/2019

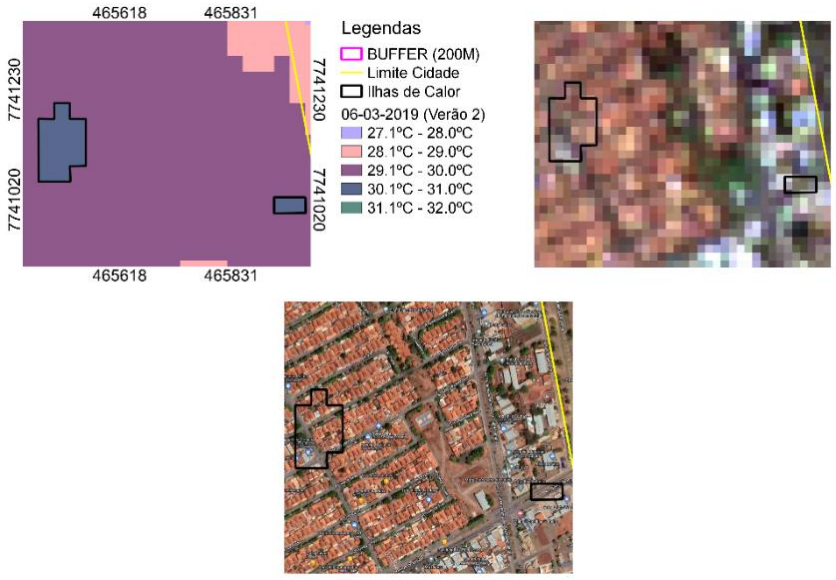

Source: Prepared by the author.

Figure 2625Map of Urban Heat Islands in Ilha Solteira – SP, on 03/06/2019

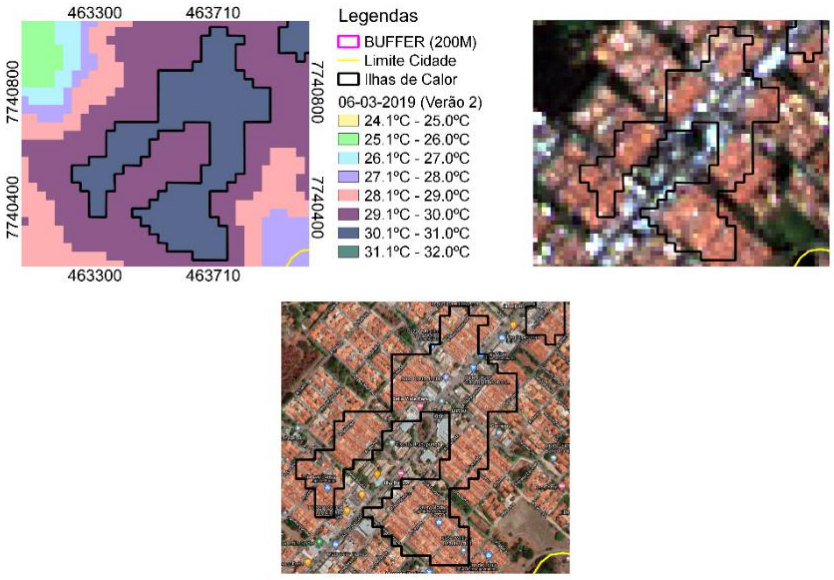

Source: Prepared by the author.

Figure 26: Map of Urban Heat Islands in Ilha Solteira – SP, on 03/06/2019

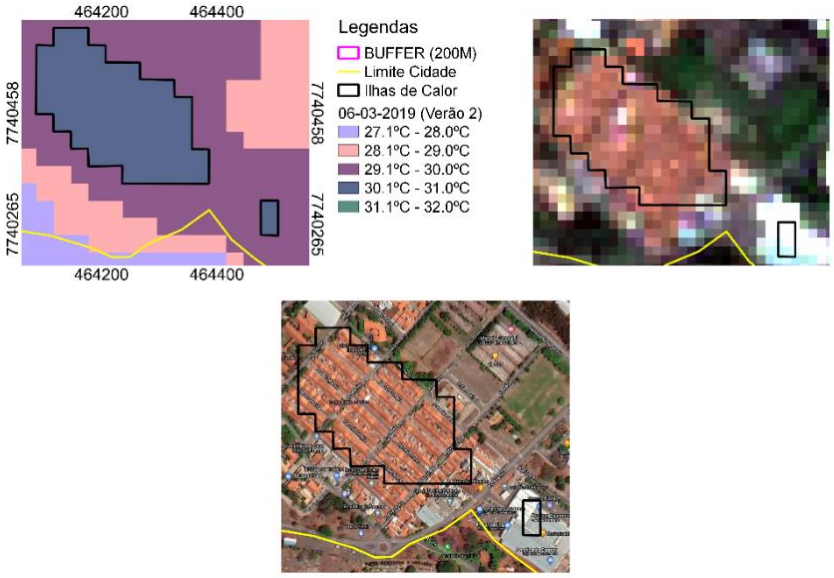

Source: Prepared by the author.

Figure 27: Map of Urban Heat Islands in Ilha Solteira – SP, on 03/06/2019

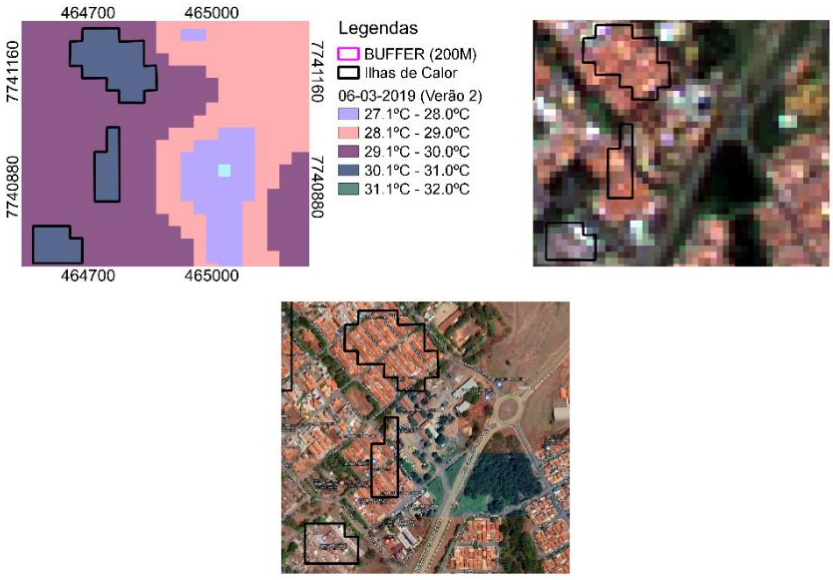

Source: Prepared by the author.

Figure 2928Map of Urban Heat Islands in Ilha Solteira – SP, on 03/06/2019

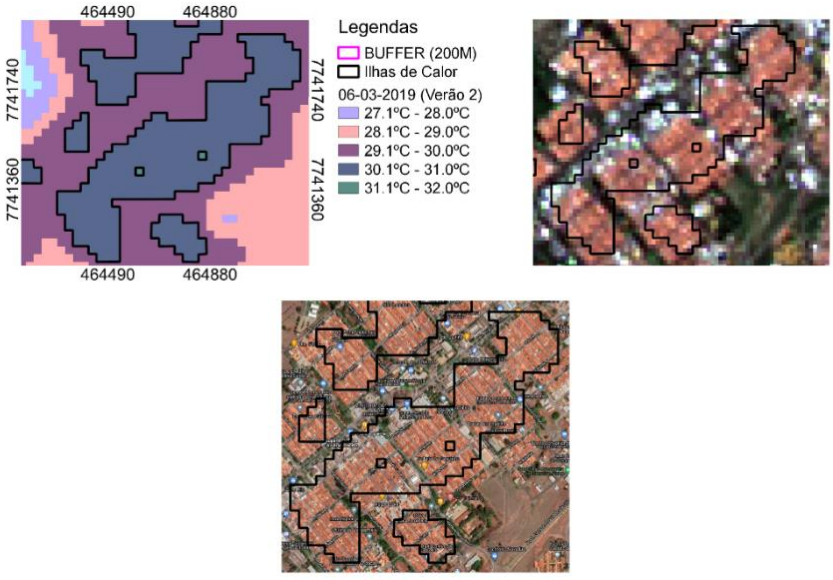

Source: Prepared by the author.

Figure 29: Map of Urban Heat Islands in Ilha Solteira – SP, on 03/06/2019

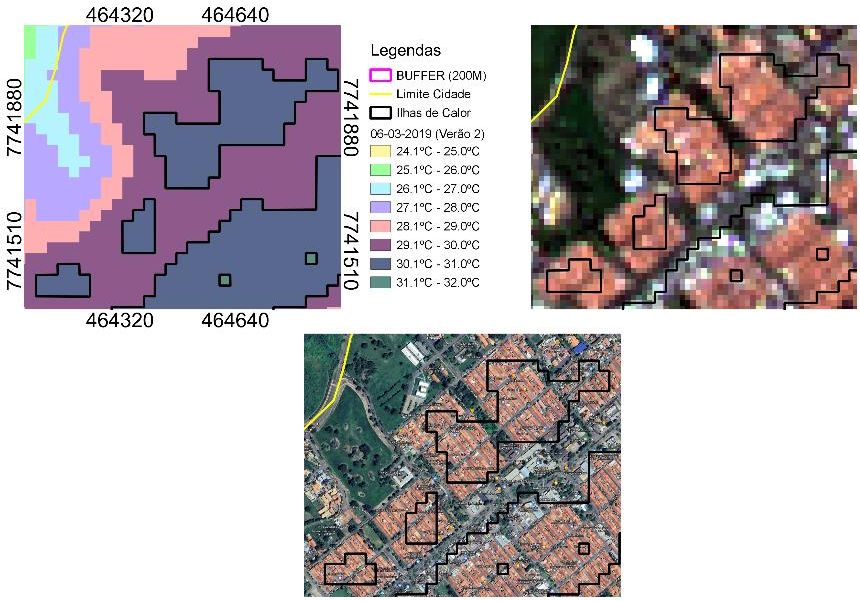

Source: Prepared by the author.

Figure 30: Map of Urban Heat Islands in Ilha Solteira – SP, on 03/06/2019

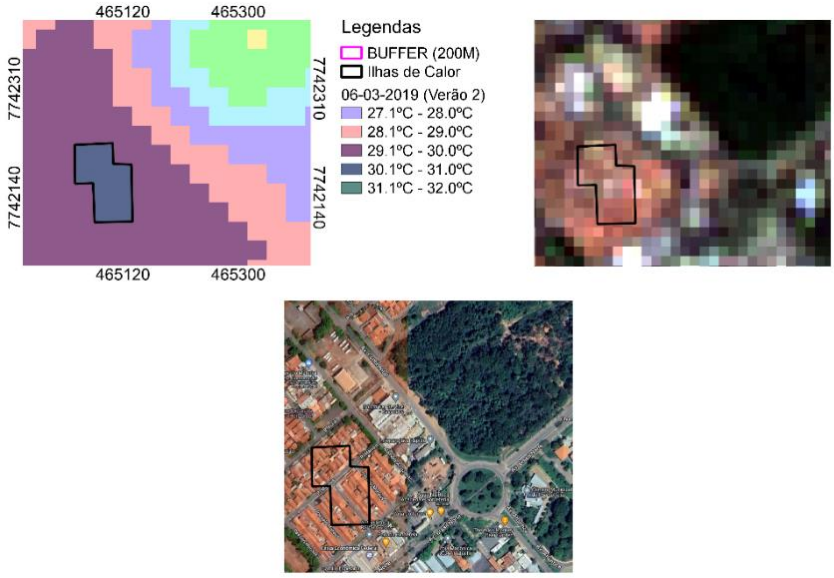

Source: Prepared by the author.
2019

4.9 WINTER 1

4.9.1 Urban Heat Island on 28/07/2019

According to the data obtained on 07/28/2019 (Figure 32), 1 area with heat islands was identified within the urban perimeter, called Areas 1. The area within the limit of 200m (surroundings) used as a reference for the identification of the ICU was under the temperature of 31.1 to 32°C.

Location: Av. Quine de Outubro, Al. Rio de Janeiro

Figure 31: Map of Urban Heat Islands in Ilha Solteira – SP, on 07/28/2019

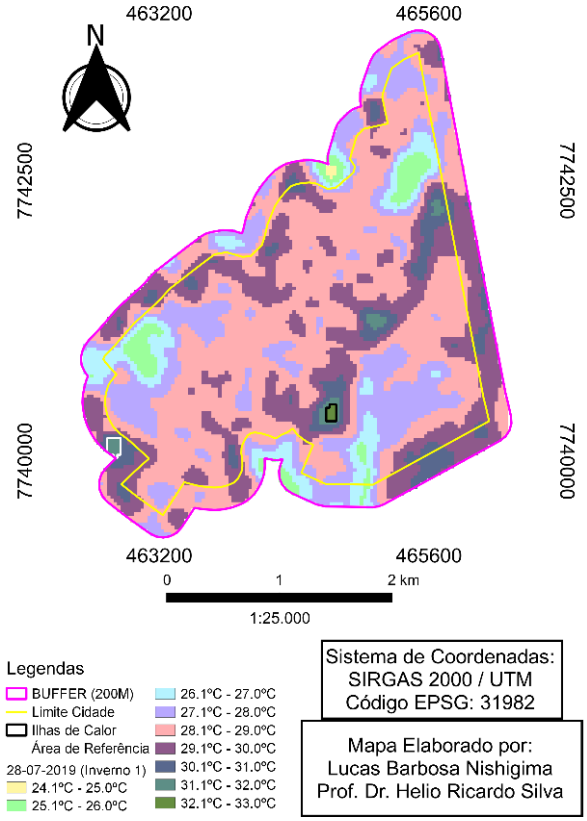

Source: Prepared by the author.

Table 8: ICU area measurements as of 07/28/2019

	Winter (1)		
	Heat Islands		
32.1ºC - 34.0ºC	Urban Boundary	Areas ICU	TOTAL
Area (ha)	734,913	1,26	736,173
Area (%)	99,83	0,17	100

Figure 32: Map of Urban Heat Islands in Ilha Solteira – SP, on 07/28/2019

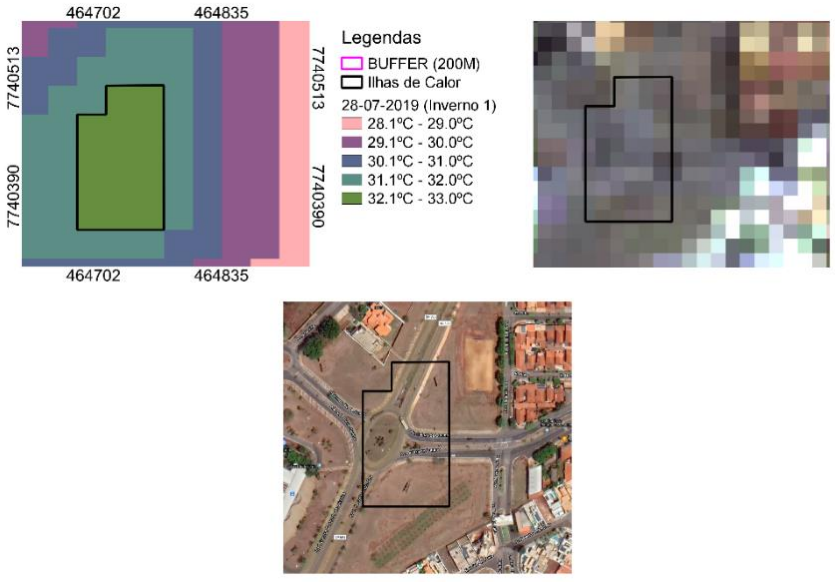

Source: Prepared by the author.

4.10 WINTER 2

4.10.1 Urban Heat Island on 07/09/2019

According to data obtained on 09/07/2019 (Figure 34), 1 area with heat islands within the urban perimeter was identified, called Areas 1. The area within the limit of 200m (surroundings) used as a reference for the identification of the ICU was under the temperature of 35.1 to 36°C.

Location: Av. Perimetral (near Praça das Araras)

Figure 33: Map of Urban Heat Islands in Ilha Solteira – SP, on 09/07/2019

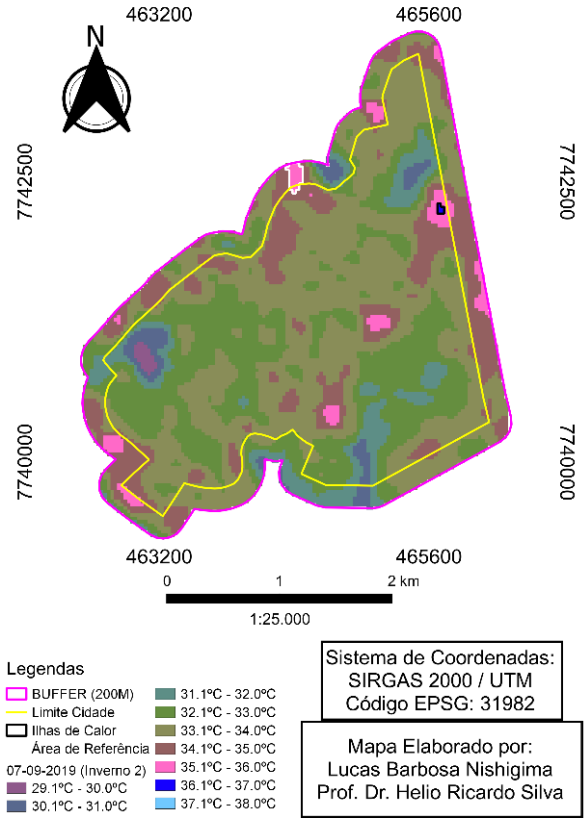

Source: Prepared by the author.

Table 9: ICU area measurements as of 09/07/2019

	Winter (2)		
	Heat Islands		
32.1ºC - 34.0ºC	Urban Boundary	Áreas ICU	TOTAL
Area (ha)	734,913	0,45	735,363
Area (%)	99,94	0,06	100

Figure 34: Map of Urban Heat Islands in Ilha Solteira – SP, on 09/07/2019

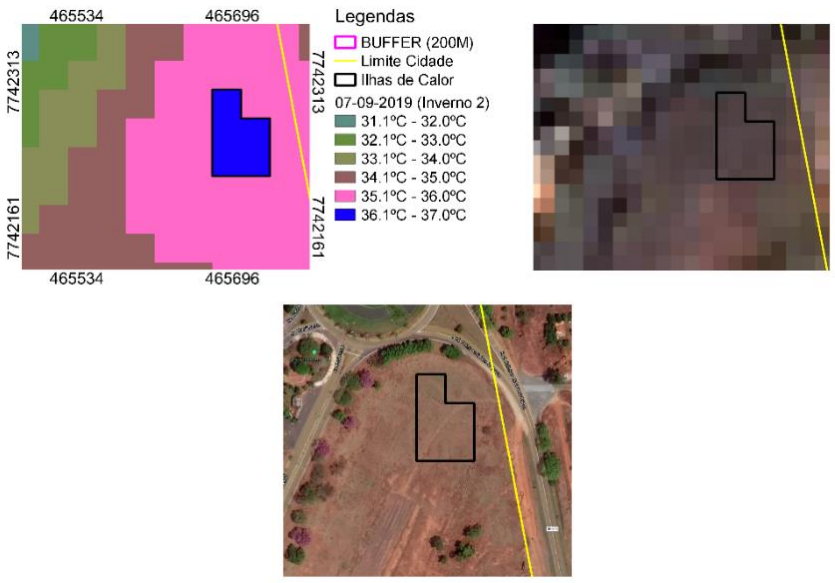

Source: Prepared by the author.

4.11 FALL 1

4.11.1 Urban Heat Island on 31/03/2019

According to data obtained on 03/31/2019 (Figure 36), 6 areas with heat islands were identified within the urban perimeter, called Areas 1, 2, 3, 4, 5, 6. The area within the 200m limit (surroundings) used as a reference for the identification of UCI was under the temperature of 33.1 to 34°C.

Location: Pas. Tijucas, R. Tijucas, Pas. Limeira, R. Limeira, Pas. Ilhéus, R. Juazeiro, Pas. Willow, Rod. Gerson Dourado de Oliveira, Pas. Olinda, R. Olinda, Pas. Forest, forest.

Figure 35: Map of Urban Heat Islands in Ilha Solteira – SP, on 03/31/2019

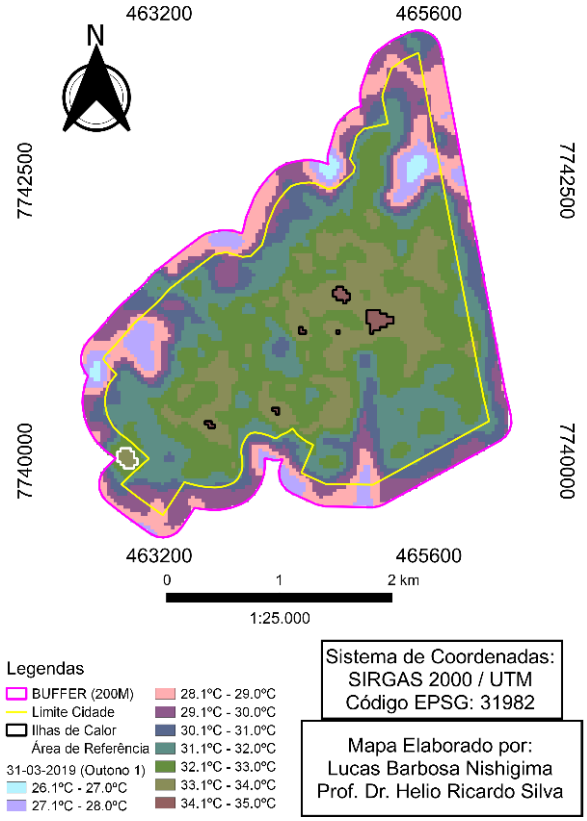

Source: Prepared by the author.

Table 10: ICU area measurements as of 03/31/2019

	Fall (1)		
	Heat Islands		
32.1ºC - 34.0ºC	Urban Boundary	Areas ICU	TOTAL
Area (ha)	734,913	5,583	740,496
Area (%)	99,24	0,76	100

Figure 36: Map of Urban Heat Islands in Ilha Solteira – SP, on 03/31/2019

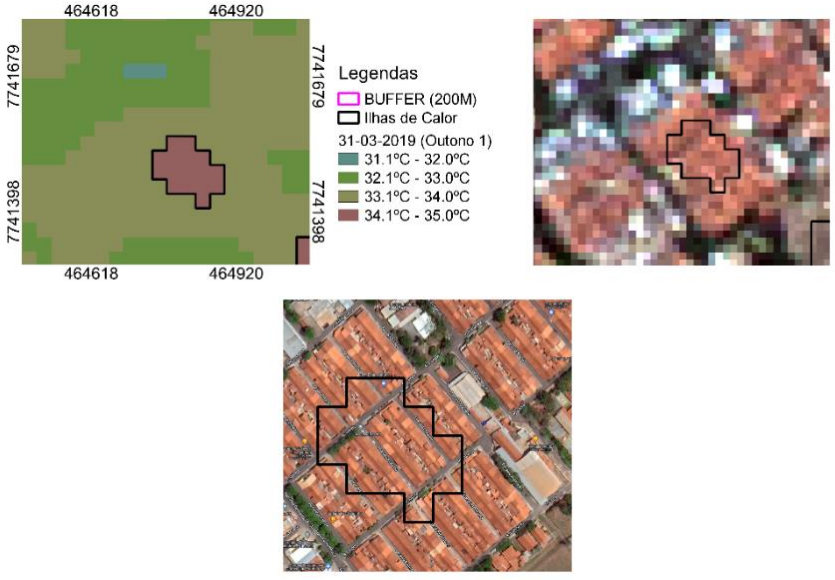

Source: Prepared by the author.

Figure 37: Map of Urban Heat Islands in Ilha Solteira – SP, on 03/31/2019

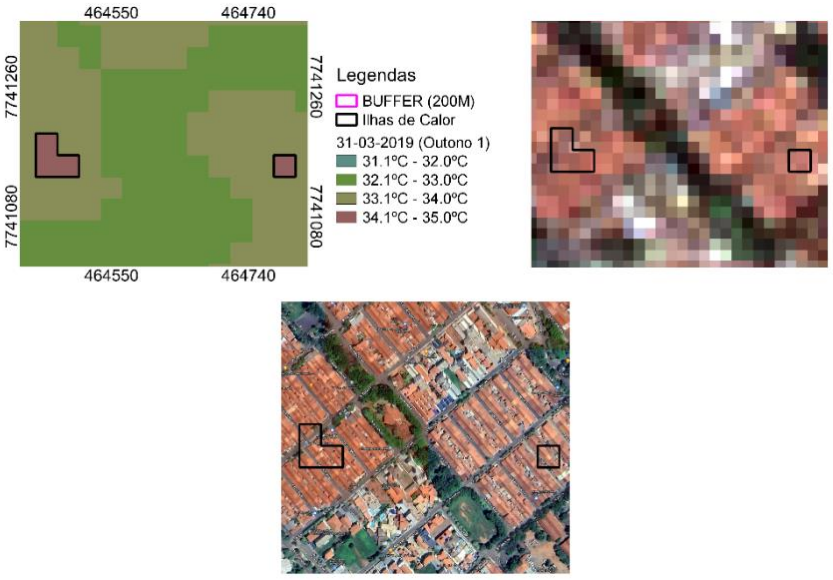

Source: Prepared by the author.

Figure 3938Map of Urban Heat Islands in Ilha Solteira – SP, on 03/31/2019

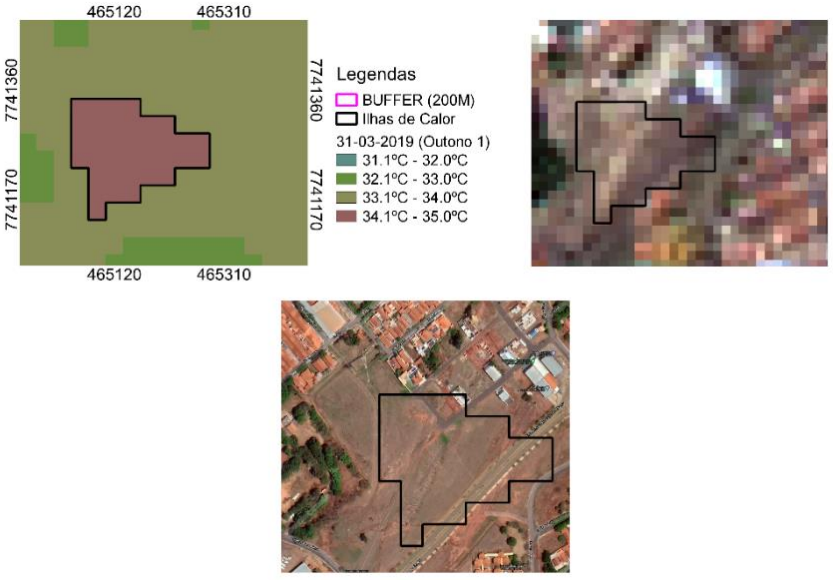

Source: Prepared by the author.

Figure 39: Map of Urban Heat Islands in Ilha Solteira – SP, on 03/31/2019

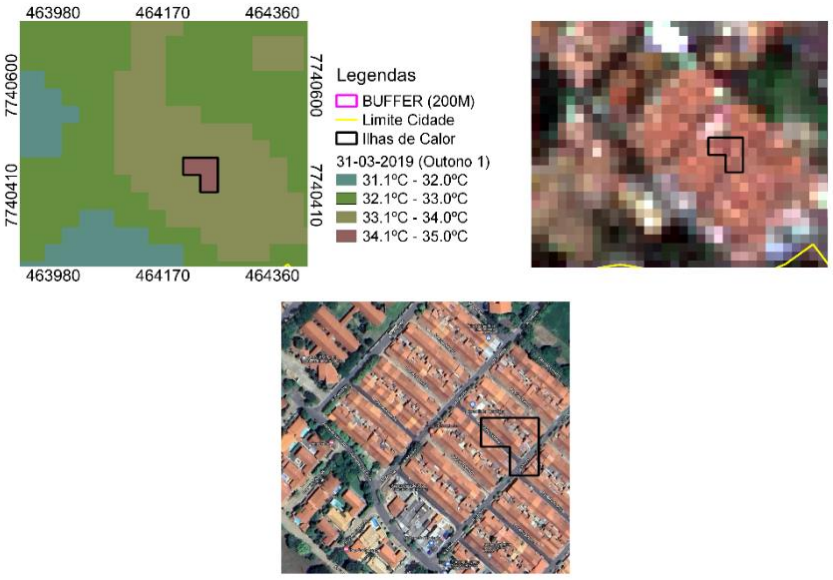

Source: Prepared by the author.

Figure 40: Map of Urban Heat Islands in Ilha Solteira – SP, on 03/31/2019

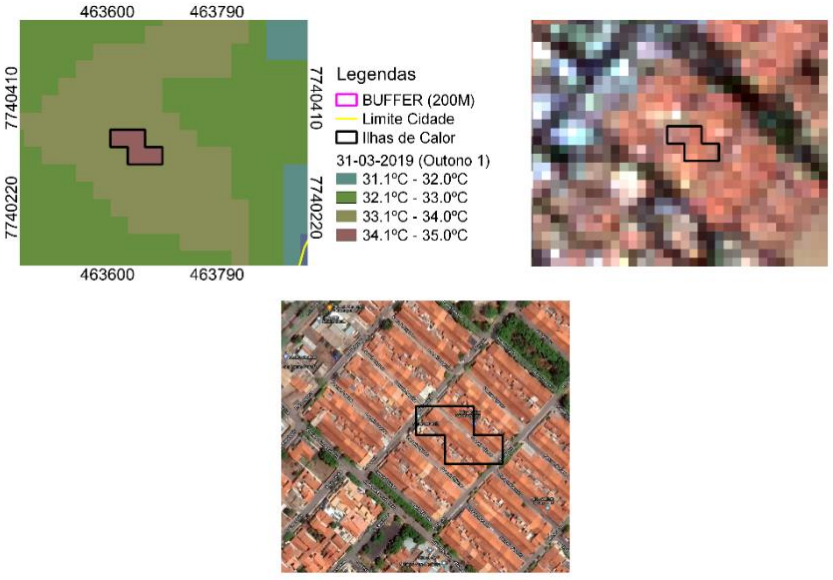

Source: Prepared by the author.

4.12 FALL 2

4.12.1 Urban Heat Island on 10/06/2019

According to data obtained on 06/10/2019 (Figure 42), no areas with heat islands were identified within the urban perimeter.

Figure 41: Map of Urban Heat Islands in Ilha Solteira – SP, on 06/10/2019

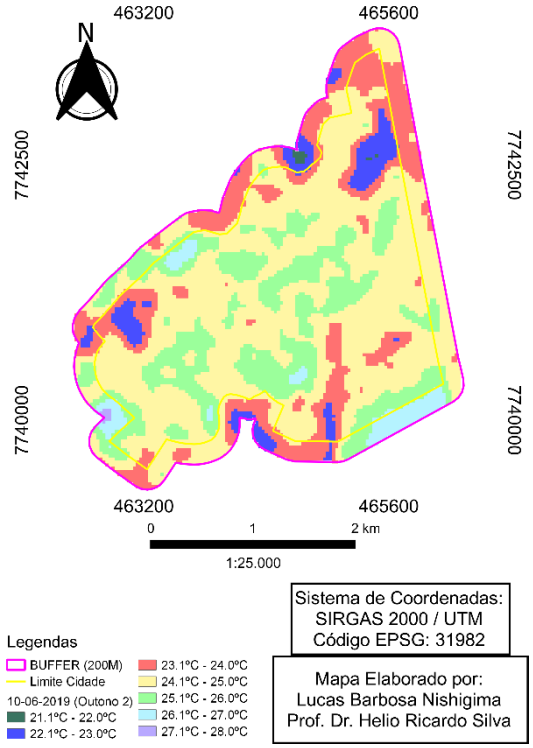

Source: Prepared by the author.

4.13 SPRING 1

4.13.1 Urban Heat Island on 25/10/2019

According to data obtained on 10/25/2019 (Figure 43), 7 areas with heat islands were identified within the urban perimeter, named as Areas 1, 2, 3, 4, 5, 6 and 7. The area within the 200m limit (surroundings) used as a reference for the identification of UCI was under the temperature of 38.1 to 39°C.

Location: Pas. Tijucas, R. Tijucas, Pas. Limeira, R. Limeira, Pas. Marilia, Marília, Av. Fifteenth of October, Pas. Salvador, R. Salvador, Pas. Juazeiro, R. Juazeiro, Pas. Ilhéus, Pas. Recife, R. Recife, Pas. Floresta, R. Floreta, R. Olinda, R. Fortaleza, Pas. Sobral

Figure 42: Map of Urban Heat Islands in Ilha Solteira – SP, on 10/25/2019

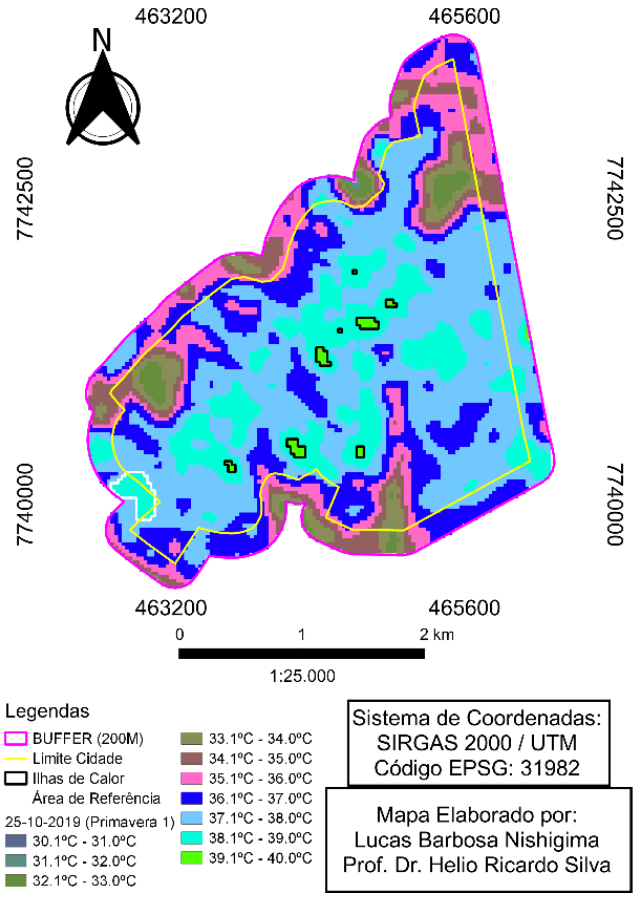

Source: Prepared by the author.

Table 11: ICU area measurements as of 10/25/2019

	Spring (1)		
	Heat Islands		
32.1ºC - 34.0ºC	Urban Boundary	Areas ICU	TOTAL
Area (ha)	734,913	5,938	740,851
Area (%)	99,19	0,81	100

Figure 43: Map of Urban Heat Islands in Ilha Solteira – SP, on 10/25/2019

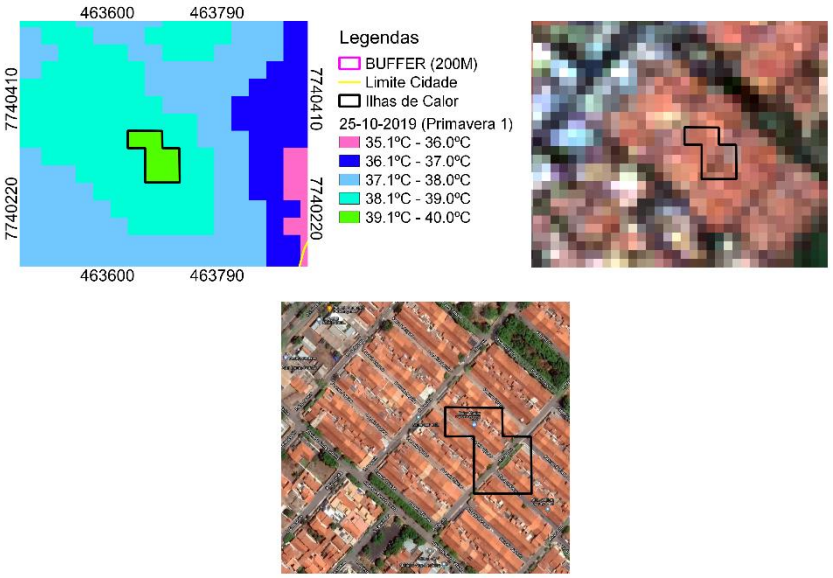

Source: Prepared by the author.

Figure 44: Map of Urban Heat Islands in Ilha Solteira – SP, on 10/25/2019

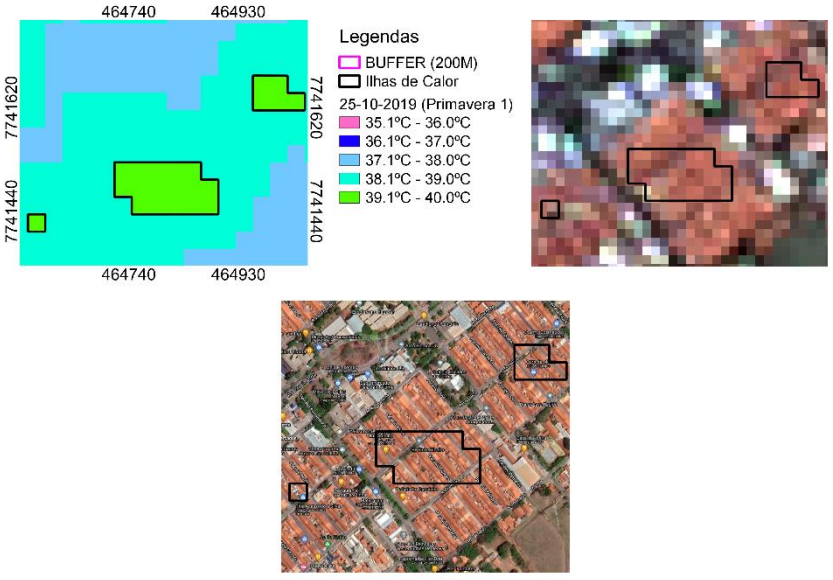

Source: Prepared by the author.

Figure 45: Map of Urban Heat Islands in Ilha Solteira – SP, on 10/25/2019

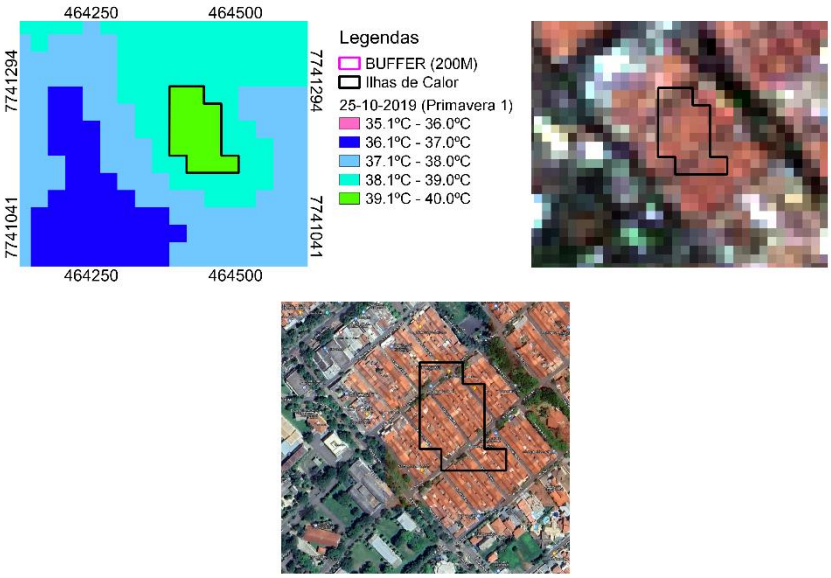

Source: Prepared by the author.

Figure 46: Map of Urban Heat Islands in Ilha Solteira – SP, on 10/25/2019

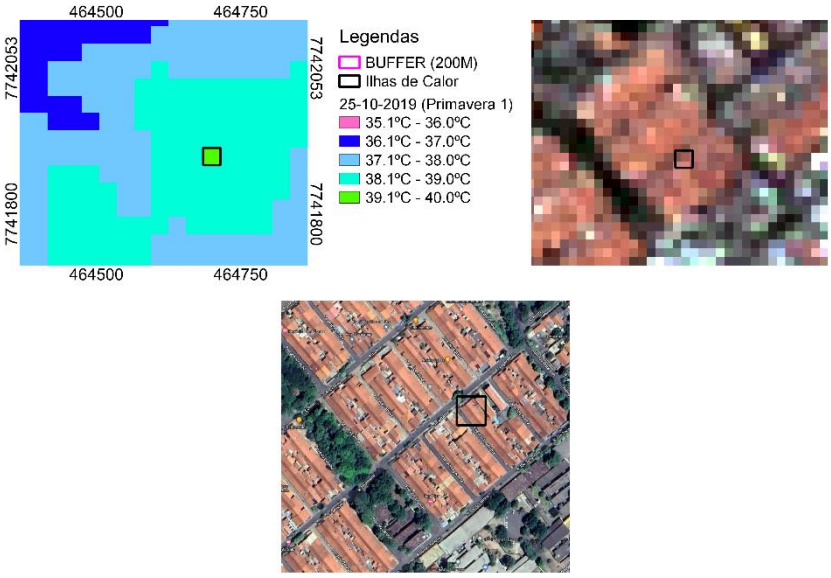

Source: Prepared by the author.

Figure 47: Map of Urban Heat Islands in Ilha Solteira – SP, on 10/25/2019

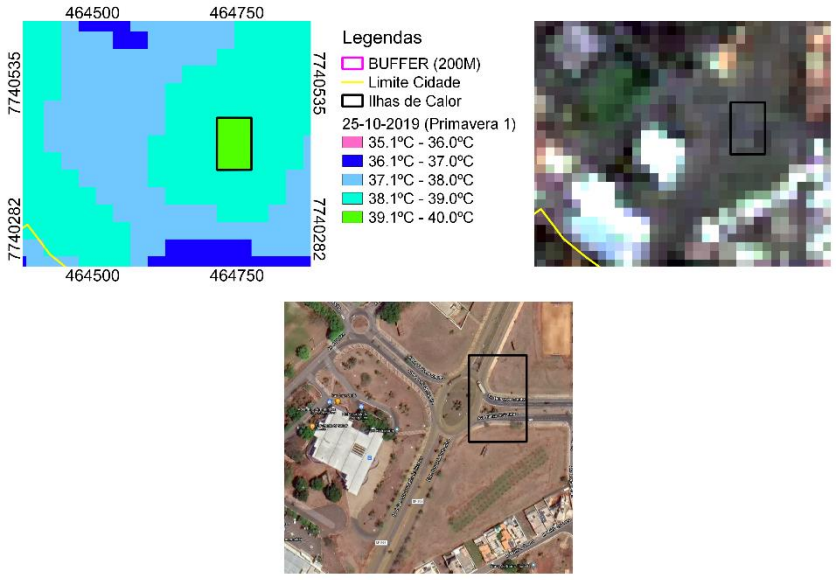

Source: Prepared by the author.

4.14 SPRING 2

4.14.1 Urban Heat Island on 17/11/2019

According to the data obtained on 11/17/2019 (Figure 49), 1 area with heat islands within the urban perimeter was identified, called Areas 1. The area within the 200m limit (surroundings) used as a reference for the identification of the UCI was under the temperature of 42.1 to 43°C.

Location: Av. Fifteenth of October

Figure 48: Map of Urban Heat Islands in Ilha Solteira – SP, on 10/25/2019

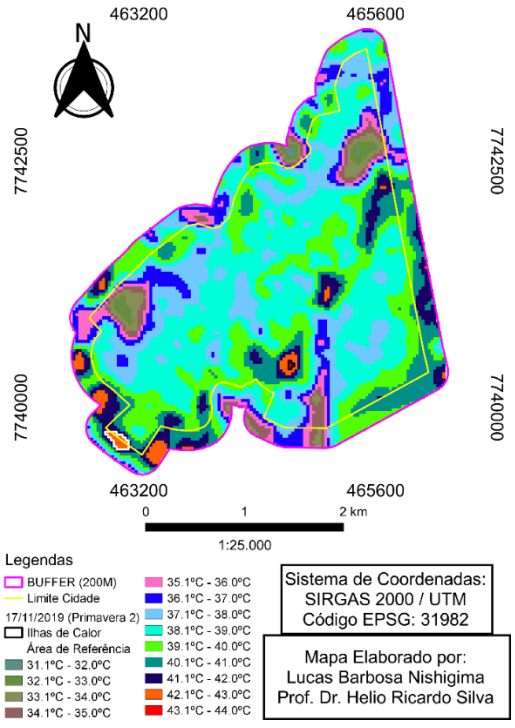

Source: Prepared by the author.

Table 12: ICU Area Measurements as of 11/17/2019

	Spring (2)		
	Heat Islands		
32.1ºC - 34.0ºC	Urban Boundary	Areas ICU	TOTAL
Area (ha)	734,913	0,36	735,273
Area (%)	99,95	0,05	100

Figure 49: Map of Urban Heat Islands in Ilha Solteira – SP, on 11/17/2019

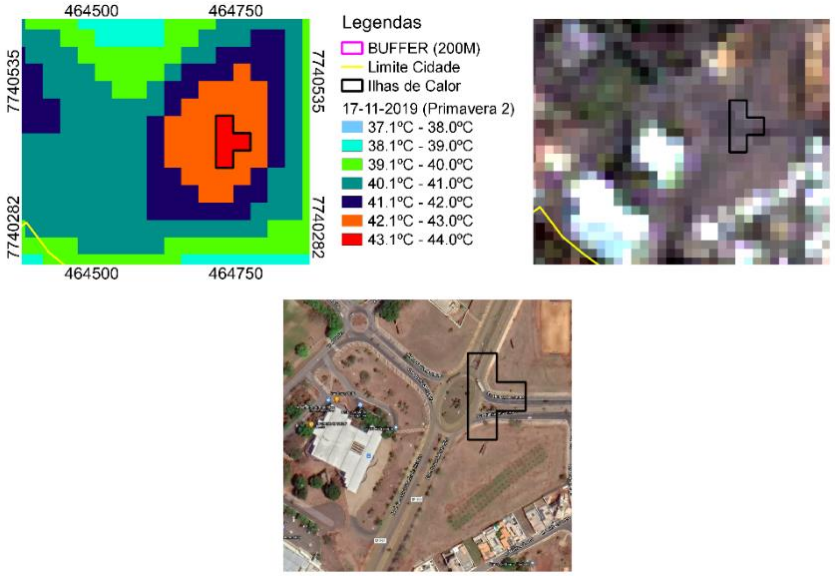

Source: Prepared by the author.

4.15 SUMMER 1

4.15.1 Urban Heat Island on 14/02/2020

According to data obtained on 02/14/2020 (Figure 51), no areas with heat islands were identified within the urban perimeter.

Figure 50: Map of Urban Heat Islands in Ilha Solteira – SP, on 02/14/2020

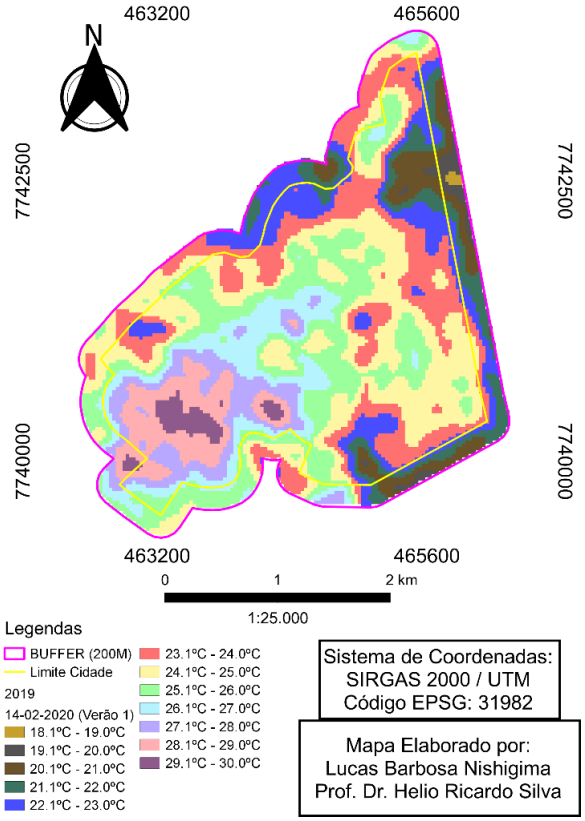

Source: Prepared by the author.

4.16 SUMMER 2

4.16.1 Urban Heat Island on 17/03/2020

According to data obtained on 03/17/2020 (Figure 52), no area with heat islands was identified within the urban perimeter.

Figure 51: Map of Urban Heat Islands in Ilha Solteira – SP, on 03/17/2020

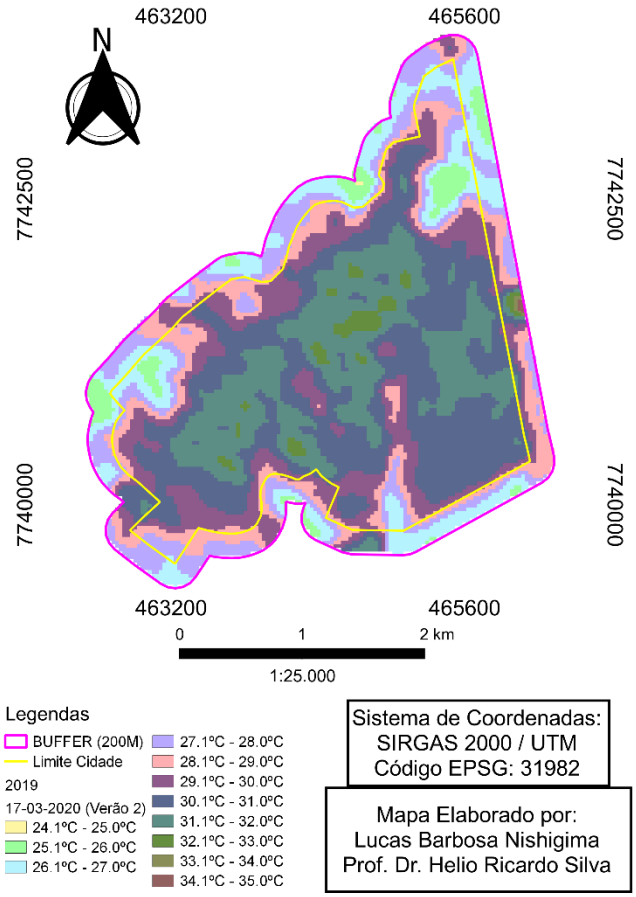

Source: Prepared by the author.
2020

4.17 WINTER 1

4.17.1 Urban Heat Island on 08/08/2020

According to the data obtained on 08/08/2020 (Figure 53), 1 area with heat islands was identified within the urban perimeter, called Areas 1. The area within the limit of 200m (surroundings) used as a reference for the identification of the ICU was under the temperature of 32.1 to 33°C.

Location: Av. Fifteenth of October

Figure 52: Map of Urban Heat Islands in Ilha Solteira – SP, on 08/08/2020

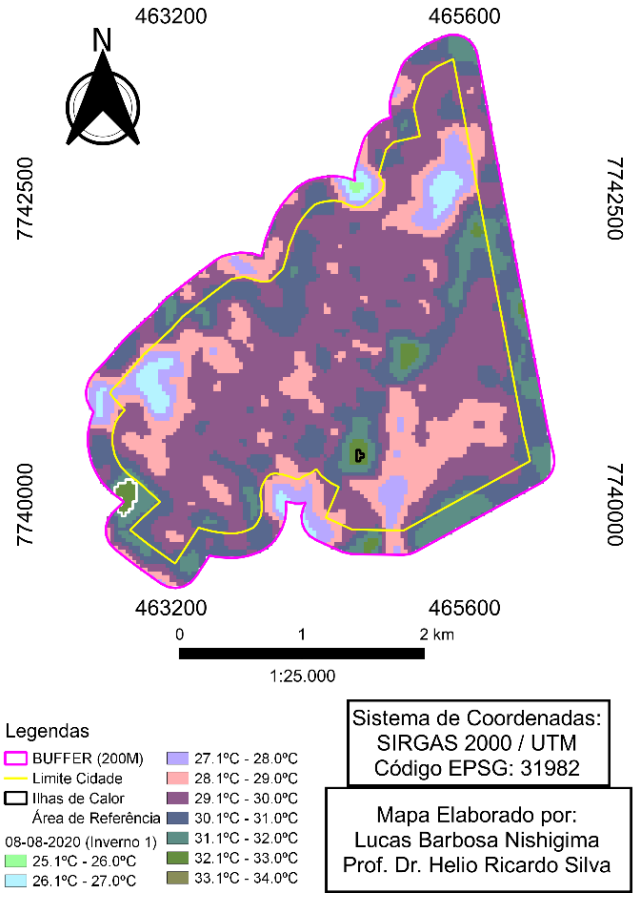

Source: Prepared by the author.

Table 13: ICU area measurements as of 08/08/2020

	Winter (1)		
	Heat Islands		
33.1ºC - 34.0ºC	Urban Boundary	Areas ICU	TOTAL
Area (ha)	734,913	0,36	735,273
Area (%)	99,95	0,05	100

Figure 53: Map of Urban Heat Islands in Ilha Solteira – SP, on 08/08/2020

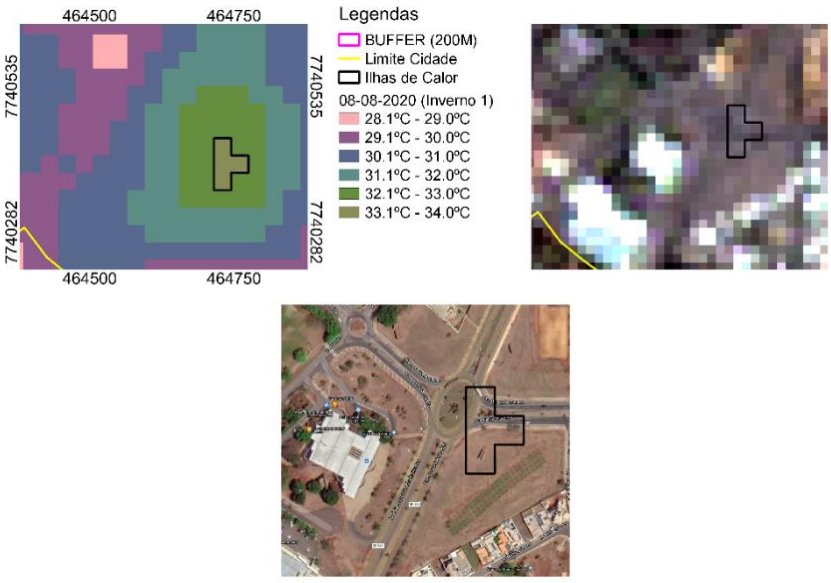

Source: Prepared by the author.

4.18 WINTER 2

4.18.1 Urban Heat Island on 16/09/2020

According to data obtained on 09/16/2020 (Figure 55), no area with heat islands was identified within the urban perimeter.

Figure 54: Map of Urban Heat Islands in Ilha Solteira – SP, on 09/16/2020

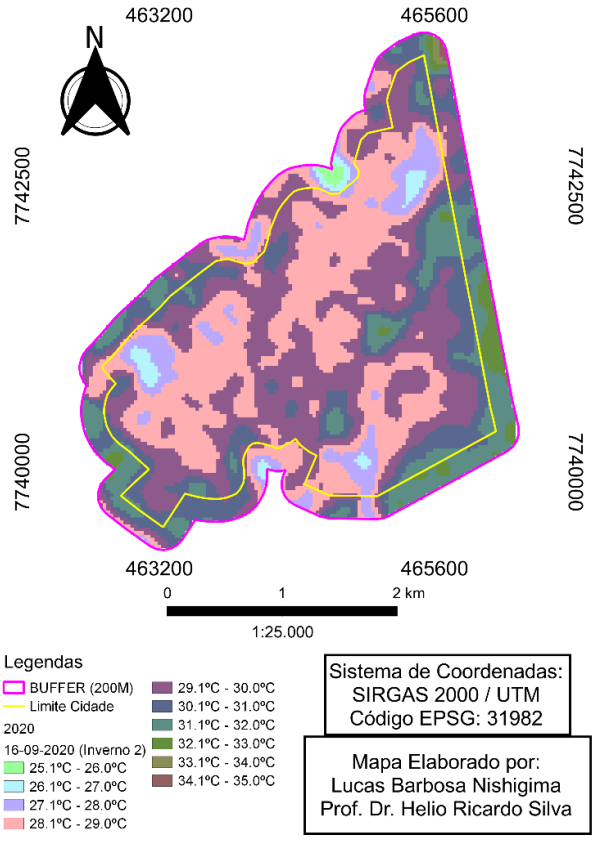

Source: Prepared by the author.

4.19 FALL 1

4.19.1 Urban Heat Island on 20/05/2020

According to the data obtained on 05/20/2020 (Figure 56), 2 areas with heat islands were identified within the urban perimeter, called Areas 1 and 2. The area within the limit of 200m (surroundings) used as a reference for the identification of the ICU was under the temperature of 29.1 to 30°C.

Location: Av. Fifteenth of October, Rod. Gerson Dourado de Oliveira

Figure 55: Map of Urban Heat Islands in Ilha Solteira – SP, on 05/20/2020

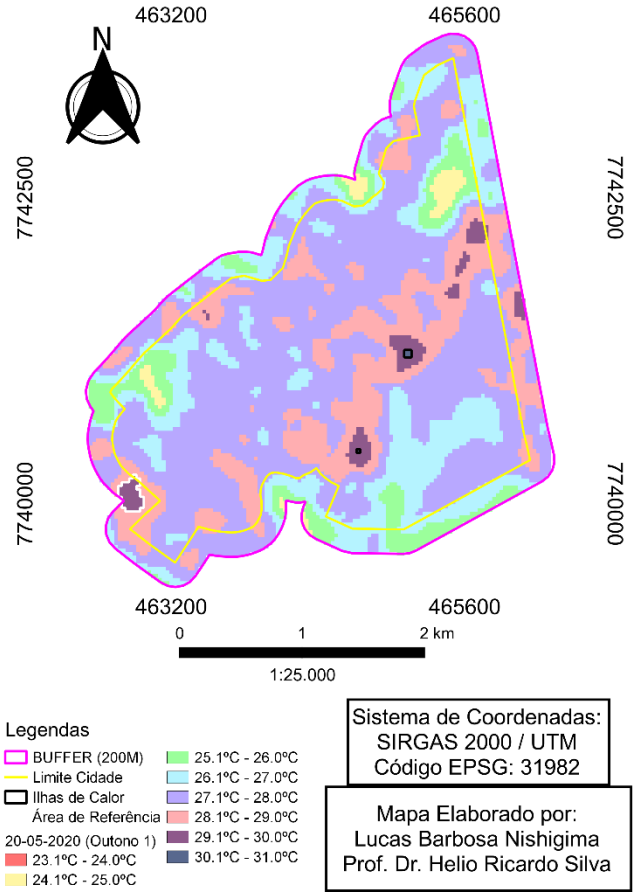

Source: Prepared by the author.

Table 14: ICU area measurements as of 05/20/2020

	Fall (1)		
	Heat Islands		
30.1ºC - 31.0ºC	Urban Boundary	Areas ICU	TOTAL
Area (ha)	734,913	0,451	735,364
Area (%)	99,94	0,06	100

Figure 56: Map of Urban Heat Islands in Ilha Solteira – SP, on 05/20/2020

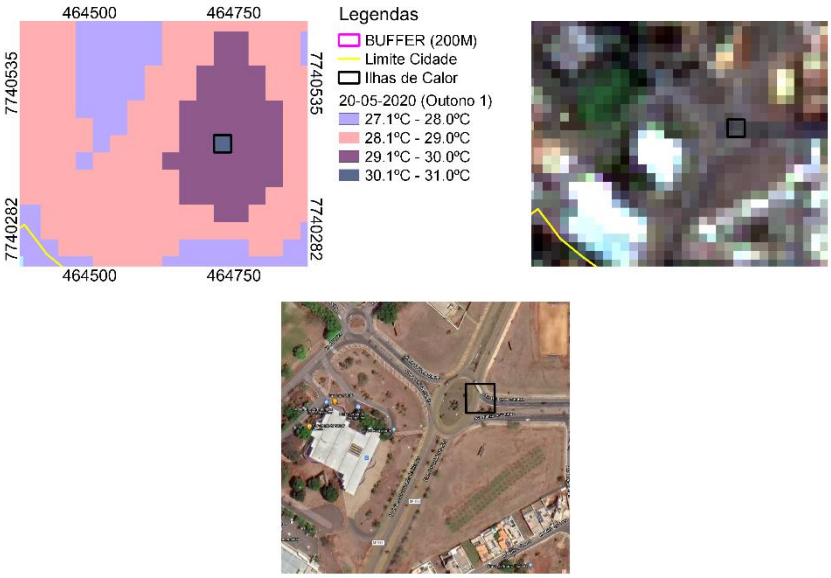

Source: Prepared by the author.

Figure 57: Map of Urban Heat Islands in Ilha Solteira – SP, on 05/20/2020

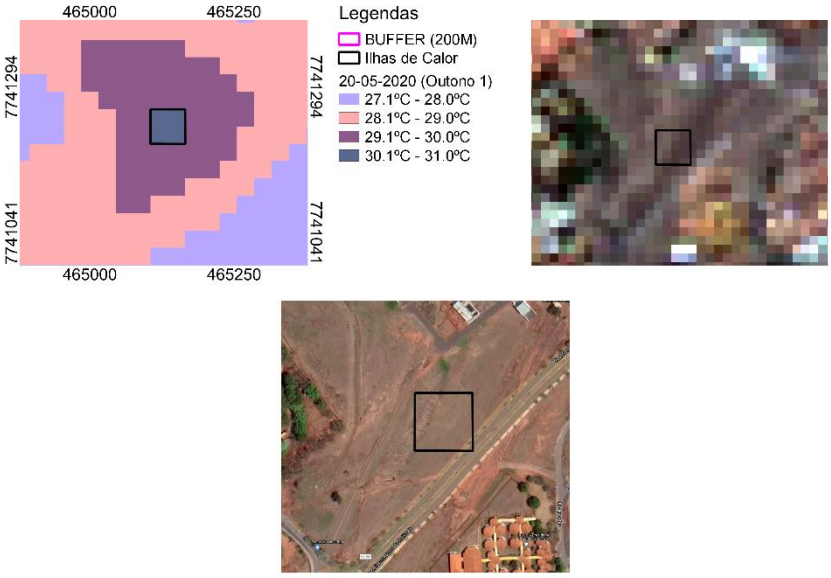

Source: Prepared by the author.

4.20 FALL 2

4.20.1 Urban Heat Island on 21/06/2020

According to the data obtained on 06/21/2020 (Figure 59), no area with heat islands was identified within the urban perimeter.

Figure 58: Map of Urban Heat Islands in Ilha Solteira – SP, on 06/21/2020

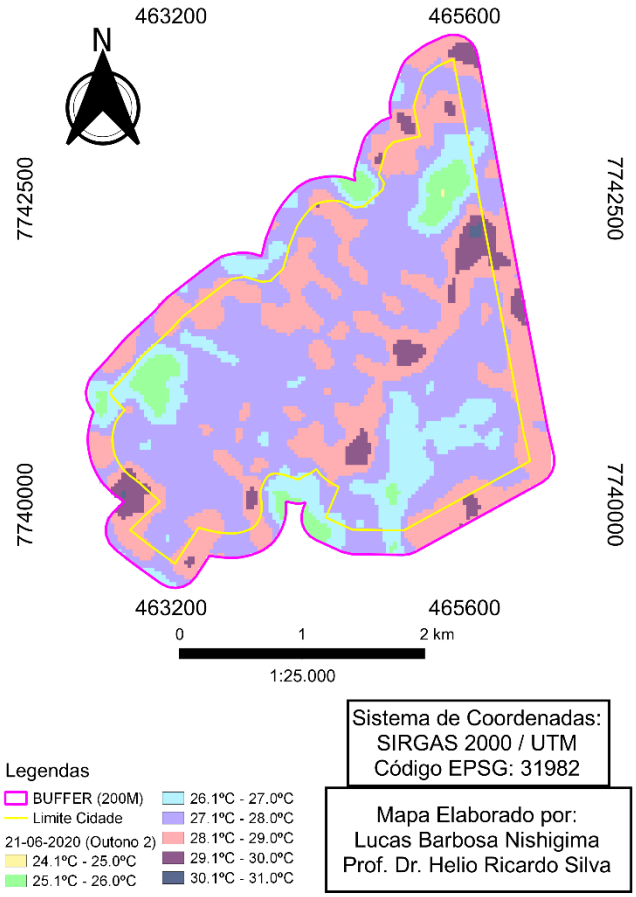

Source: Prepared by the author.

4.21 SPRING 1

4.21.1 Urban Heat Island on 11/10/2020

According to data obtained on 10/11/2020 (Figure 60), no area with heat islands was identified within the urban perimeter.

Figure 59: Map of Urban Heat Islands in Ilha Solteira – SP, on 10/11/2020

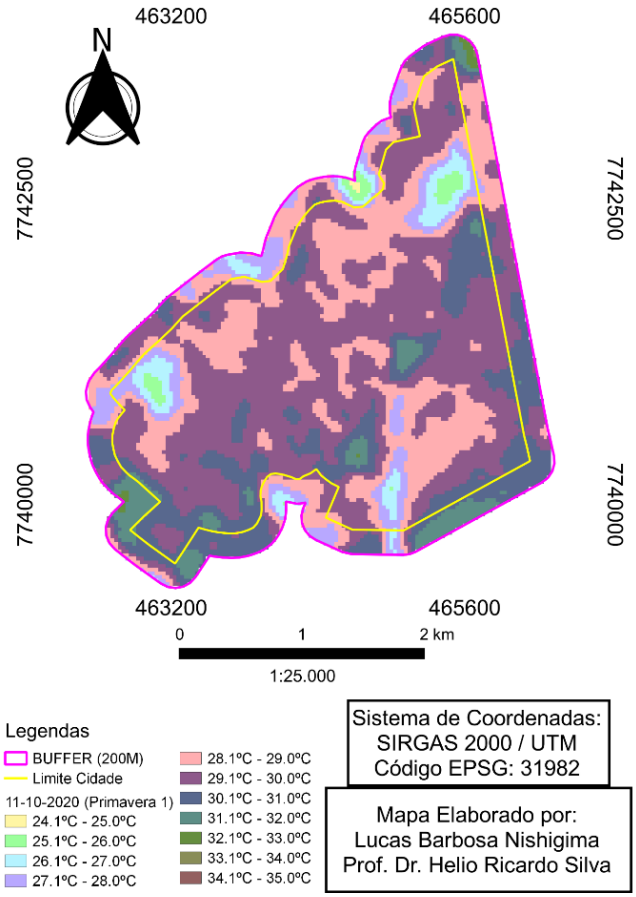

Source: Prepared by the author.

4.22 SPRING 2

4.22.1 Urban Heat Island on 28/11/2020

According to data obtained on 11/28/2020 (Figure 61), no area with heat islands was identified within the urban perimeter.

Figure 60: Map of Urban Heat Islands in Ilha Solteira – SP, on 11/26/2020

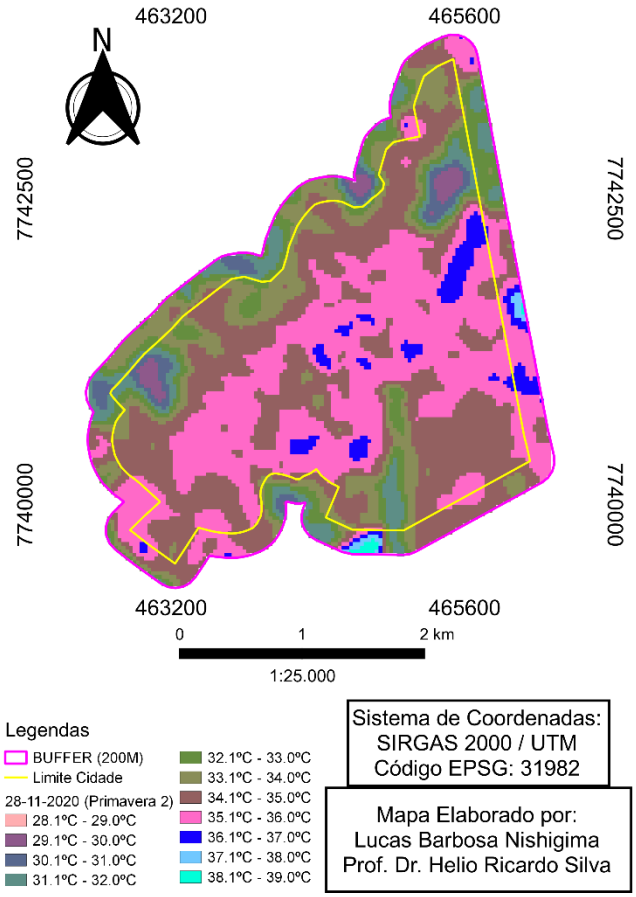

Source: Prepared by the author.

4.23 SUMMER 1

4.23.1 Urban Heat Island on 07/02/2021

According to data obtained on 02/07/2021 (Figure 62), no area with heat islands was identified within the urban perimeter.

Figure 61: Map of Urban Heat Islands in Ilha Solteira – SP, on 02/07/2021

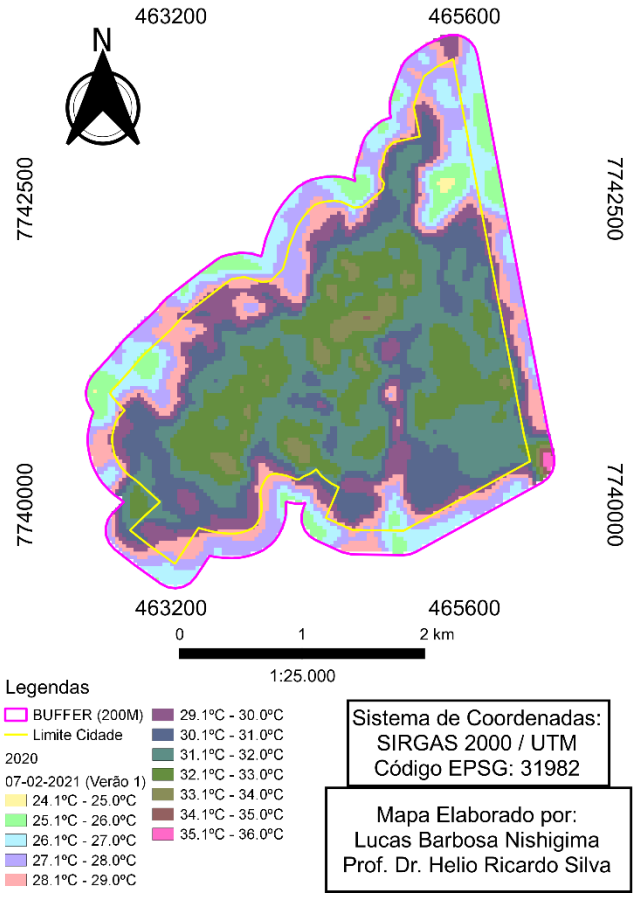

Source: Prepared by the author.

4.24 SUMMER 2

4.24.1 Urban Heat Island on 23/02/2021

According to data obtained on 02/07/2021 (Figure 63), no area with heat islands was identified within the urban perimeter.

Figure 62: Map of Urban Heat Islands in Ilha Solteira – SP, on 02/23/2021

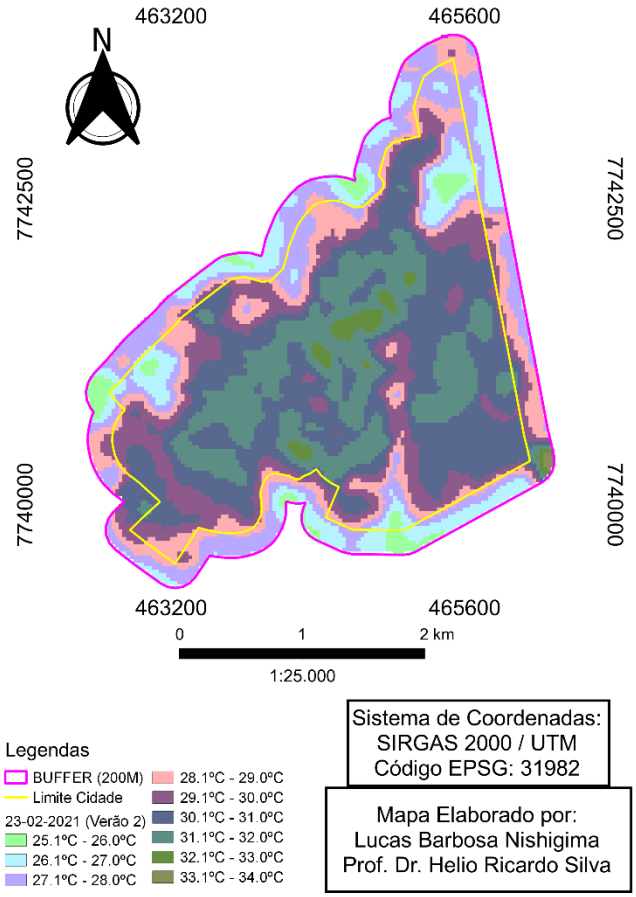

Source: Prepared by the author.
2021

4.25 WINTER 1

4.25.1 Urban Heat Island on 11/08/2021

According to data obtained on 08/11/2021 (Figure 64), no area with heat islands was identified within the urban perimeter.

Figure 63: Map of Urban Heat Islands in Ilha Solteira – SP, on 08/11/2021

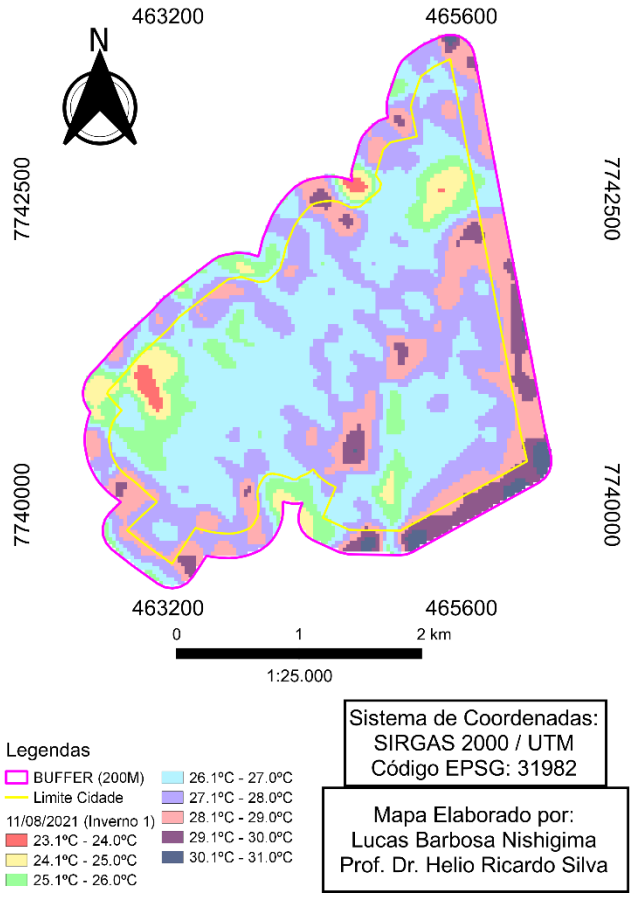

Source: Prepared by the author himself

4.26 WINTER 2

4.26.1 Urban Heat Island on 12/09/2021

According to data obtained on 09/12/2021 (Figure 65), no area with heat islands was identified within the urban perimeter.

Figure 64: Map of Urban Heat Islands in Ilha Solteira – SP, on 09/12/2021

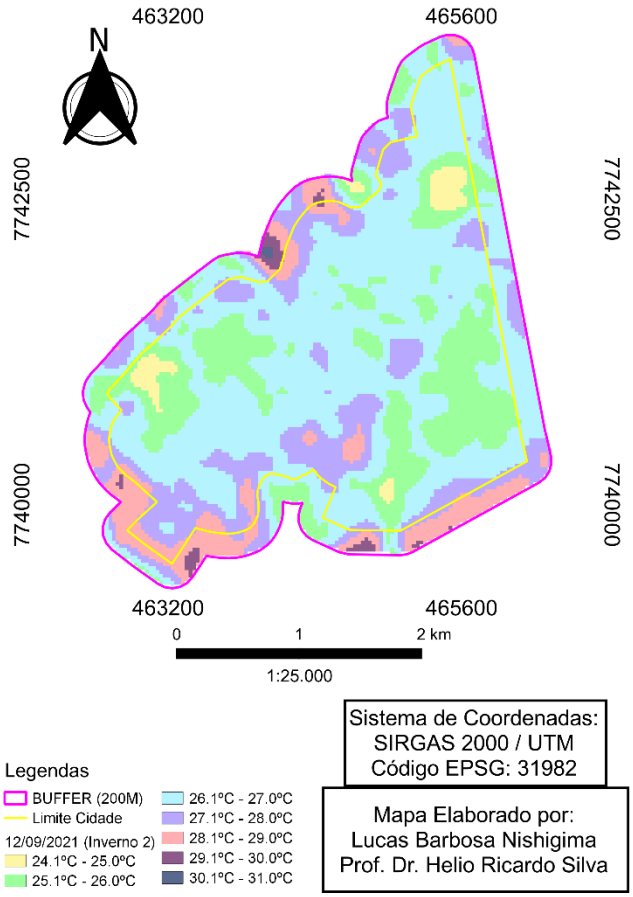

Source: Prepared by the author.

4.27 FALL 1

4.27.1 Urban Heat Island on 21/04/2021

According to data obtained on 04/21/2021 (Figure 66), no area with heat islands was identified within the urban perimeter.

Figure 65: Map of Urban Heat Islands in Ilha Solteira – SP, on 04/21/2021

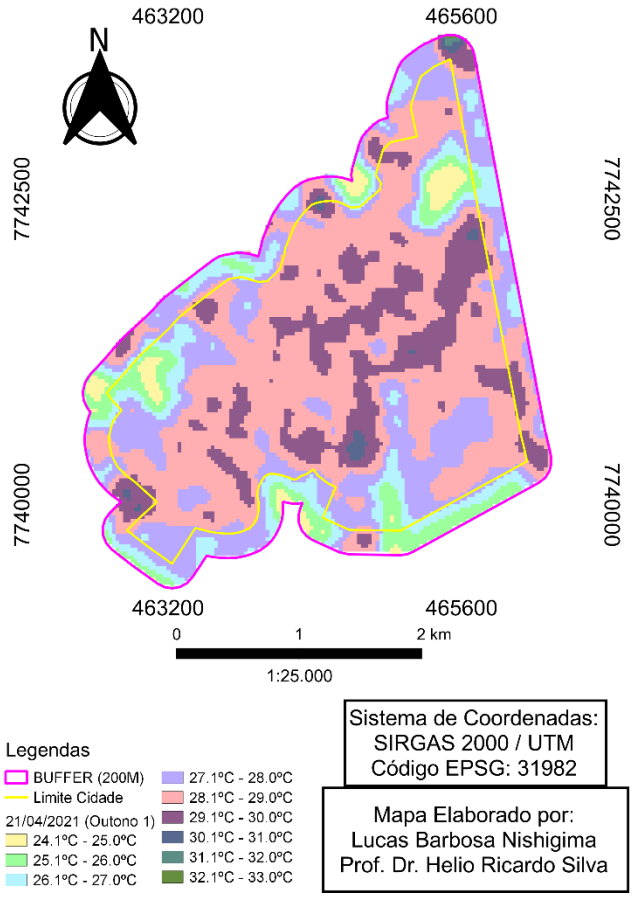

Source: Prepared by the author.

4.28 FALL 2

4.28.1 Urban Heat Island on 15/06/2021

According to data obtained on 06/15/2021 (Figure 67), no area with heat islands was identified within the urban perimeter.

Figure 66: Map of Urban Heat Islands in Ilha Solteira – SP, on 06/15/2021

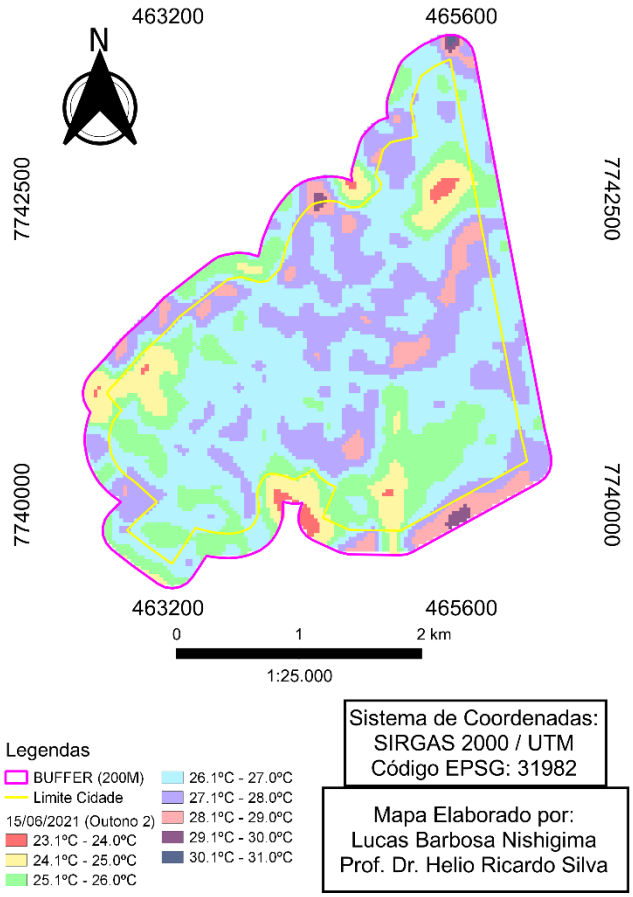

Source: Prepared by the author.

4.29 SPRING 1

4.29.1 Urban Heat Island on 06/11/2021

According to data obtained on 11/06/2021 (Figure 68), no area with heat islands was identified within the urban perimeter.

Figure 67: Map of Urban Heat Islands in Ilha Solteira – SP, on 11/06/2021

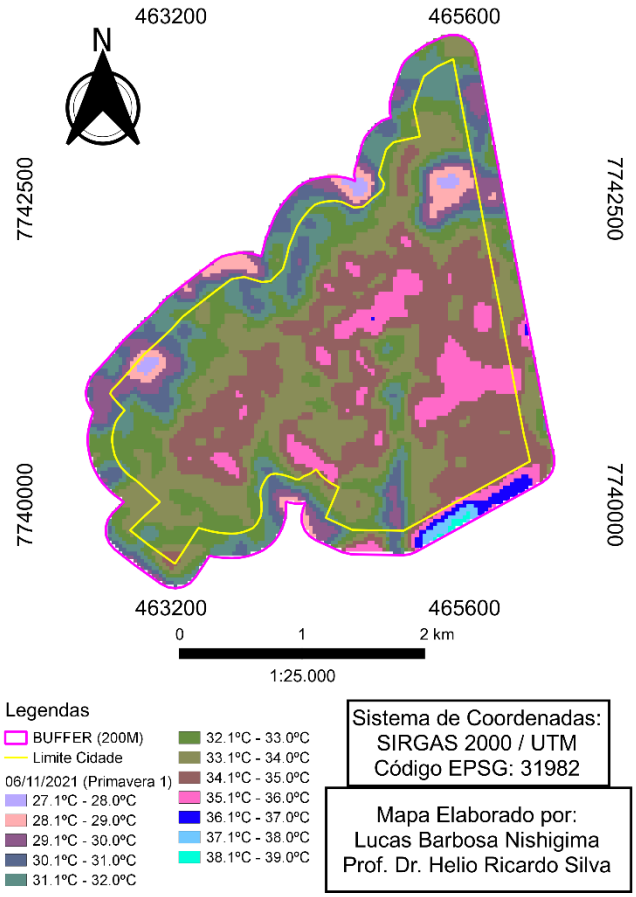

Source: Prepared by the author.

4.30 SPRING 2

4.30.1 Urban Heat Island on 08/12/2021

According to data obtained on 12/08/2021 (Figure 69), no area with heat islands was identified within the urban perimeter.

Figure 68: Map of Urban Heat Islands in Ilha Solteira – SP, on 12/08/2021

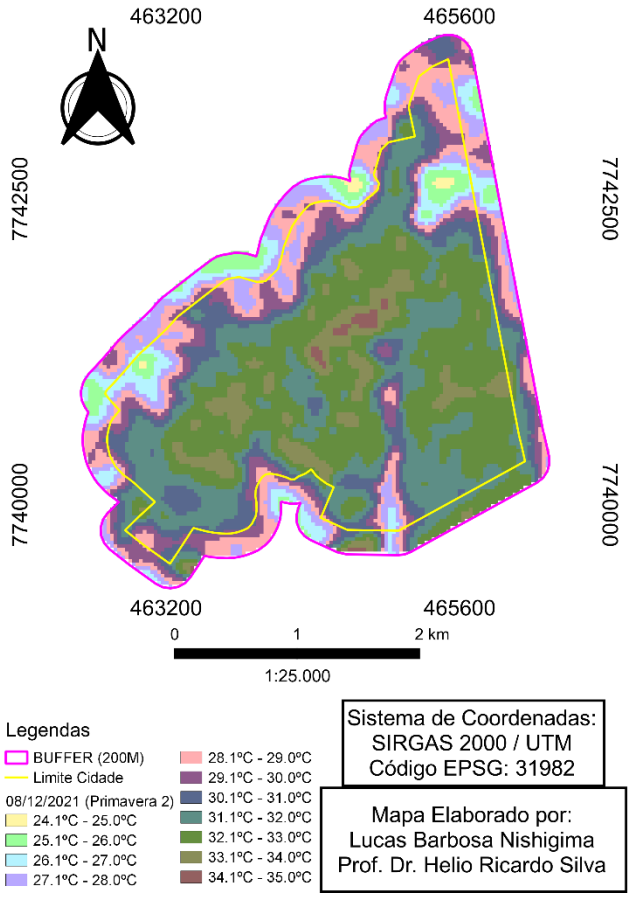

Source: Prepared by the author.

4.31 SUMMER 1

4.31.1 Urban Heat Island on 10/02/2022

According to the data obtained on 02/10/2022 (Figure 70), 7 areas with heat islands were identified within the urban perimeter, called Areas 1, 2, 3, 4, 5, 6, 7, 8, 9, 10, 11, 12, 13, 14. The area within the limit of 200m (surroundings) used as a reference for the identification of the ICU was under the temperature of 31.1 to 32°C.

Local: Pas. Laguna, R. Laguna, Pas. Tijuca, R. Tijuca, Pas. Recanto, Pas. Marilia, R. Marilia, Pas. Limeira, R. Limeira, Pas. Araras, R. Sorocaba, Pas. Sorocaba, Al. São Paulo, Pas. Santos, R. Rio Paraíba, Av. Brasil Sul, Pas. Belo Horizonte, Pas. Uberaba, R. Rio Doce, Pas. Niterói, R. Goiânia, Pas. Goiânia, Pas. Cristalina, R. Teresina, Pas. Teresina, Pas. Batalha, R. Caracol, Pas. Caracol, R. Colinas, Pas. Colinas, R. Imperatriz, Pas. Imperatriz, R. Rio Tocantins, R. Icaraí, Pas. Icaraí, Al. Ceara, Pas. Canindé, Pas. Fortaleza, R. Fortaleza, Pas. Sobral, R. Sobral, Pas. Olinda, R. Olinda, Pas. Floresta, R. Floresta, Pas. Palmares, Al. Pernambuco, R. Recife, Pas. Recife, Pas. Caruaru, R. Caruaru, Rua Salvador, Pas. Salvador, Pas. Juazeiro, R. Juazeiro, Pas. Ilhéus, Pas. Cabo, R. Cabo, Pas. Salgueiro.

Figure 69: Map of Urban Heat Islands in Ilha Solteira – SP, on 02/10/2022

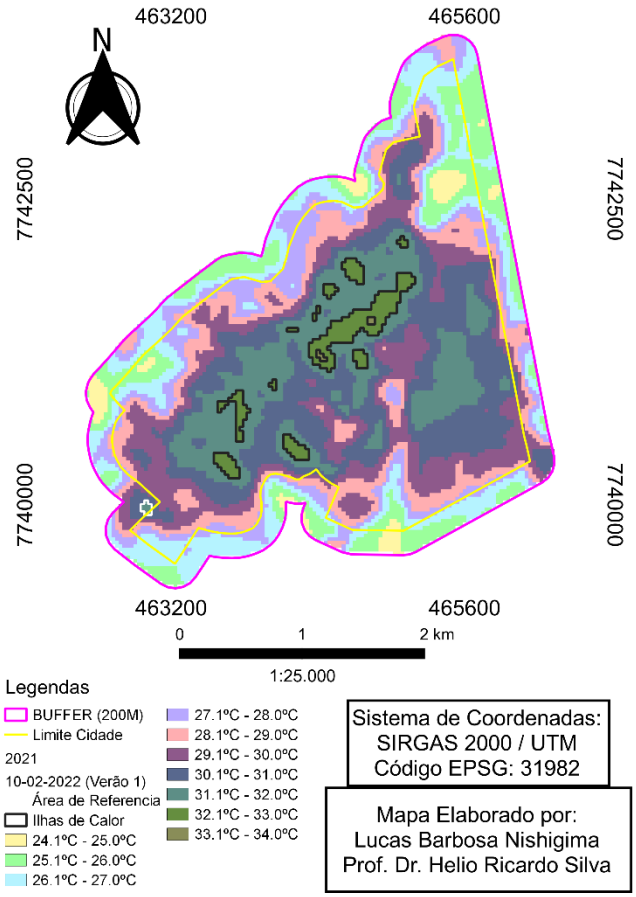

Source: Prepared by the author.

Table 18: ICU area measurements on 10/02/2022

	Summer (1)		
	Heat Islands		
33.1ºC - 34.0ºC	Urban Boundary	Areas ICU	TOTAL
Area (ha)	734,913	35,1	770,013
Area (%)	95,95	4,05	100

Figure 70: Map of Urban Heat Islands in Ilha Solteira – SP, on 02/10/2022

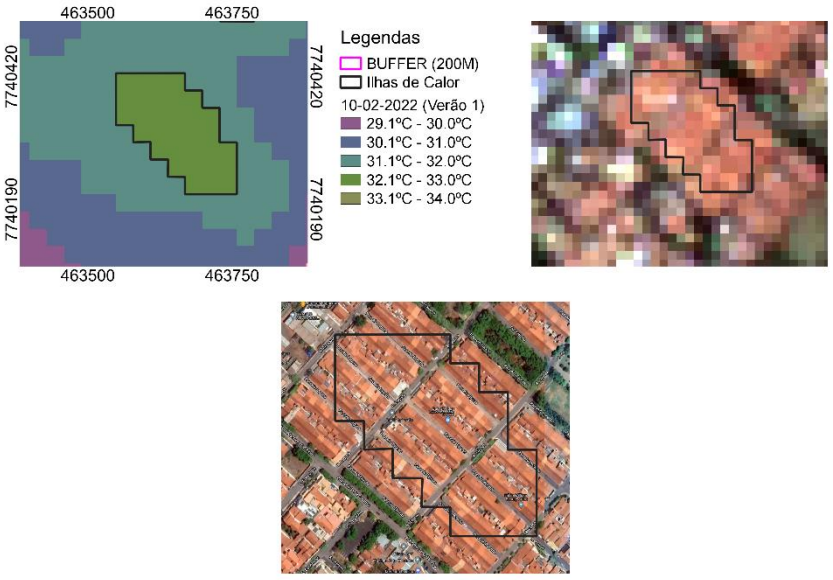

Source: Prepared by the author.

Figure 71: Map of Urban Heat Islands in Ilha Solteira – SP, on 02/10/2022

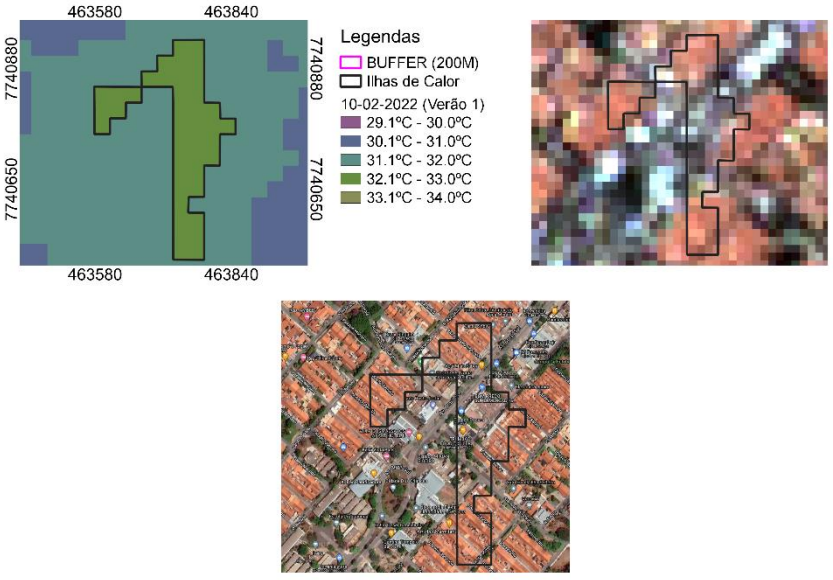

Source: Prepared by the author.

Figure 72: Map of Urban Heat Islands in Ilha Solteira – SP, on 02/10/2022

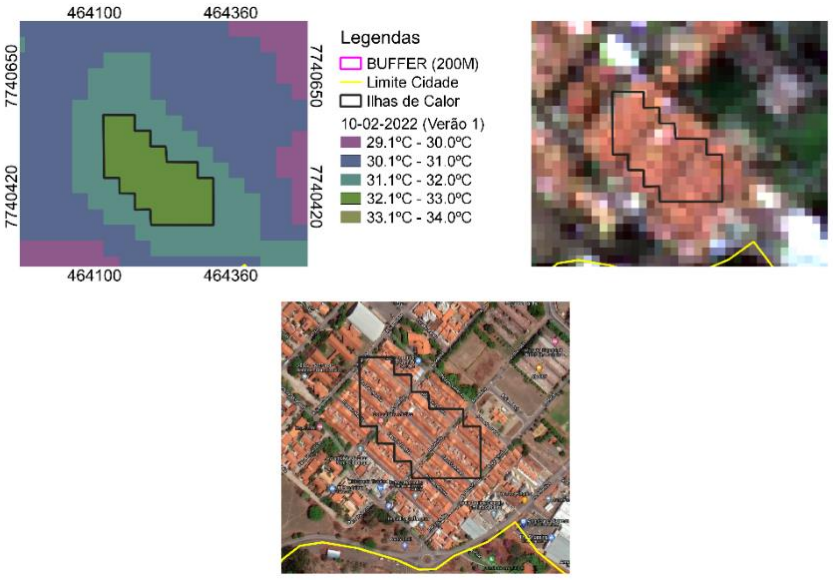

Source: Prepared by the author.

Figure 73: Map of Urban Heat Islands in Ilha Solteira – SP, on 02/10/2022

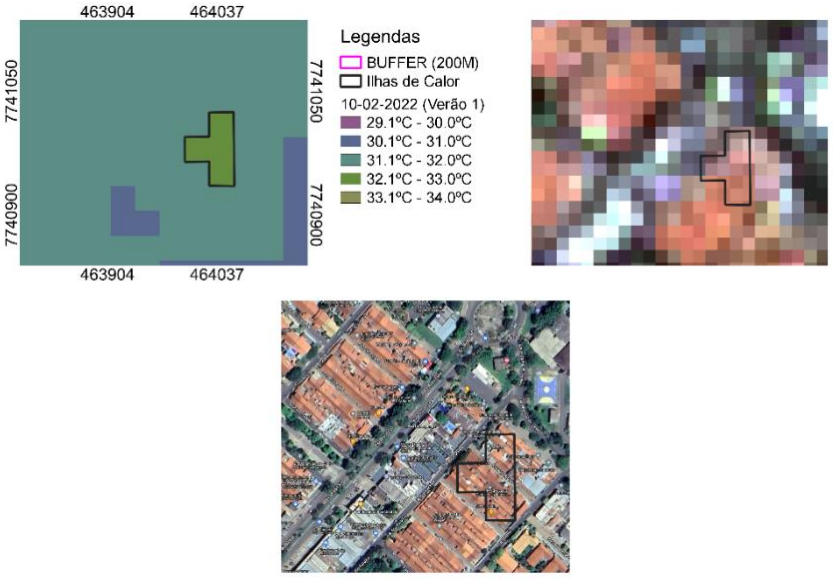

Source: Prepared by the author.

Figure 74: Map of Urban Heat Islands in Ilha Solteira – SP, on 02/10/2022

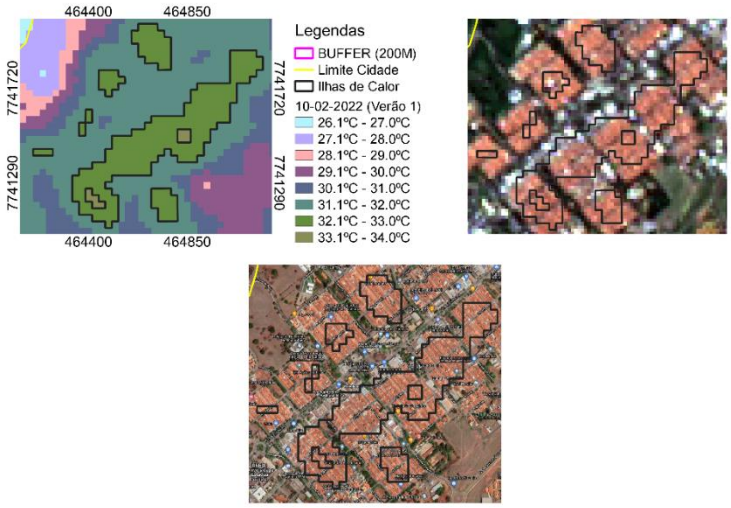

Source: Prepared by the author.

Figure 75: Map of Urban Heat Islands in Ilha Solteira – SP, on 02/10/2022

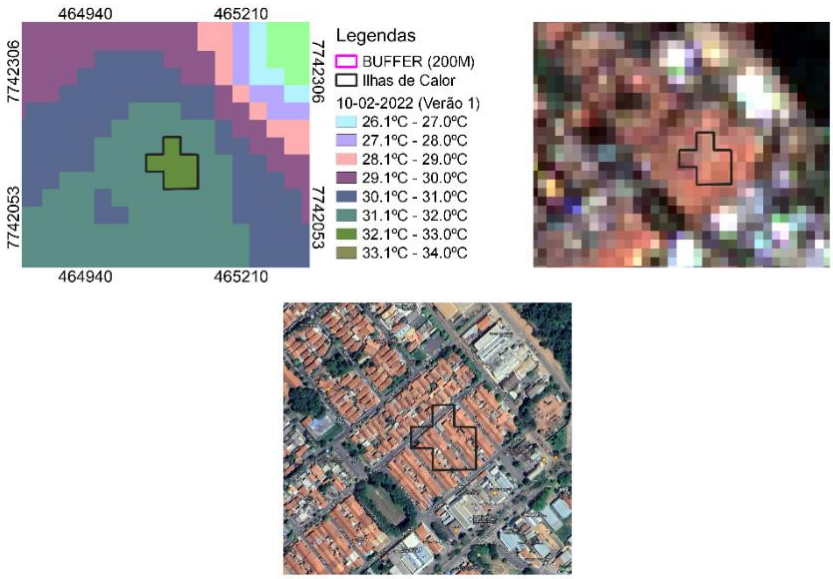

Source: Prepared by the author.

4.32 SUMMER 2

4.32.1 Urban Heat Island on 07/03/2022

According to the data obtained on 03/07/2022 (Figure 77), no area with heat islands was identified within the urban perimeter.

Figure 76: Map of Urban Heat Islands in Ilha Solteira – SP, on 03/07/2022

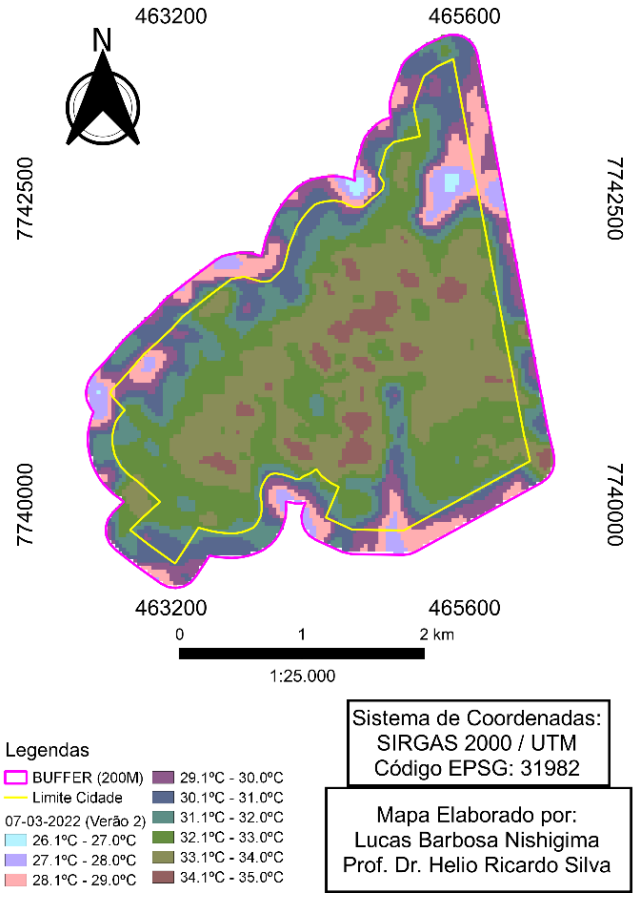

Source: Prepared by the author.

5 DISCUSSION

After the analysis of the maps, annual comparative tables and graphs were made to find out whether or not there were reductions in ICU's over the years 2018 to 2021, for this parameters such as: Number of ICU's, Wind Speed, and in which station it was identified.

For the year 2018 and 2019 in (Table 19 and 20) we can see that the ICU's were well distributed occurring from Autumn 2 to Summer (2) (2018) and in the Winter (1) to Autumn (1) and Spring (1 and 2) seasons (2019), we can say that a large part of this event may have happened because of the fires, wind speed, presence of cars and industrial activity around, and there may even be influence from other municipalities.

Table 15: Comparative Table of ICU Presence Between Stations in 2018

Year	Month	Seasons	Qty of ICU	Ampl. of ICU - ºC	ICU Magnitude	% ICU	Vel. of the wind m/s	Beaufort scale	Figure	ICU Presence
2018	August	Winter (1)	0	0	0	0	1,8	Weak	8	
2018	September	Winter (2)	0	0	0	0	1,5	Weak	9	
2018	April	Fall (1)	0	0	0	0	0,8	Weak	10	
2018	May	Fall (2)	1	1ºC	Weak	0,024	1,5	Weak	11	

2018	October	Spring (1)	3	1ºC	Weak	0,22	1,5	Weak	13	
2018	December	Spring (2)	19	2ºC	Weak	18,78	0,6	Weak	15	
2019	February	Summer (1)	1	1ºC	Weak	0,07	0,8	Weak	22	
2019	March	Summer (2)	17	2ºC	Weak	10,12	1,1	Weak	24	

*Red color: No ICUs were present
**Color Green: Presented ICU's

Table 20: Comparative table of ICU presence between 2019 seasons

Year	Month	Seasons	Qty of ICU	Ampl. of ICU - ºC	ICU Magnitude	% ICU	Vel. of the wind m/s	Beaufort scale	Figure	ICU Presence
2019	August	Winter (1)	1	1ºC	Weak	0,17	1	Weak	32	
2019	September	Winter (2)	1	1ºC	Weak	0,06	2,6	Weak	34	
2019	April	Fall (1)	6	1ºC	Weak	0,76	0,8	Weak	36	
2019	May	Fall (2)	0	0	0	0	1,8	Weak	42	
2019	October	Spring (1)	7	1ºC	Weak	4,05	0,9	Weak	43	
2019	December	Spring (2)	1	1ºC	Weak	0,05	1,8	Weak	49	
2020	February	Summer (1)	0	0	0	0	0,8	Weak	51	
2020	March	Summer (2)	0	0	0	0	0,5	Weak	52	

*Red color: No ICUs were present
**Color Green: Presented ICU's

In 2020 and 2021 (tables 21 and 22) there was a large reduction in ICU's, one of the theories is that the Covid-19 pandemic has helped to reduce greenhouse gas emissions, mainly Carbon Dioxide, which contributed to this significant reduction. Another possible theory was that the years 2020 and 2021 were an atypical year in climatology where there was no very defined time of heat and cold.

Table 16: Comparative Table of ICU presence between stations in 2020

Year	Month	Seasons	Qty of ICU	Ampl. of ICU - ºC	ICU Magnitude	% ICU	Vel. of the wind m/s	Beaufort scale	Figure	ICU Presence
2020	August	Winter (1)	1	1ºC	Weak	0,05	0,8	Weak	32	
2020	September	Winter (2)	0	0	0	0	2	Weak	34	
2020	April	Fall (1)	2	1ºC	Weak	0,06	1,3	Weak	10	
2020	May	Fall (2)	0	0	0	0	1,2	Weak	11	
2020	October	Spring (1)	0	0	0	0	1,4	Weak	13	
2020	December	Spring (2)	0	0	0	0	2,1	Weak	15	
2021	February	Summer (1)	0	0	0	0	0,6	Weak	22	
2021	March	Summer (2)	0	0	0	0	0,8	Weak	24	

*Red color: No ICUs were present
**Color Green: Presented ICU's

Table 17: Comparative Table of ICU presence between stations in 2021

Year	Month	Seasons	Qty of ICU	Ampl. of ICU - ºC	ICU Magnitude	% ICU	Vel. of the wind m/s	Beaufort scale	Figure	ICU Presence
2021	August	Winter (1)	0	0	0	0	1,4	Weak	64	
2021	September	Winter (2)	0	0	0	0	1,2	Weak	65	
2021	April	Fall (1)	0	0	0	0	1,1	Weak	66	
2021	May	Fall (2)	0	0	0	0	0,8	Weak	67	
2021	October	Spring (1)	0	0	0	0	0,3	Weak	68	

2021	December	Spring (2)	0	0	0	0	1,7	Weak	69	
2022	February	Summer (1)	1	1ºC	Weak	4,05	0,9	Weak	70	
2022	March	Summer (2)	0	0	0	0	0,5	Fraca	77	

*Red color: No ICUs were present
**Color Green: Presented ICU's

Comparing the data obtained with data previously done by other students

After analyzing the graphs, tables were made to better illustrate what was previously discussed, and the results can be seen below (Graphs 1, 2, 3 and 4).

Chart 1: Comparative Chart of the ICU for the year 2018

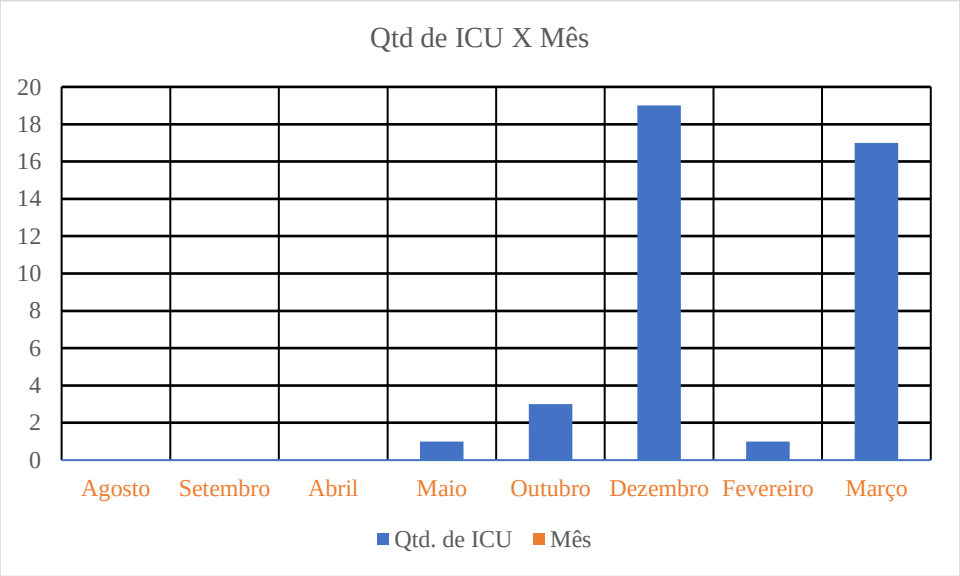

Source: Prepared by the author.

Chart 2: Comparative Chart of the ICU for the year 2019

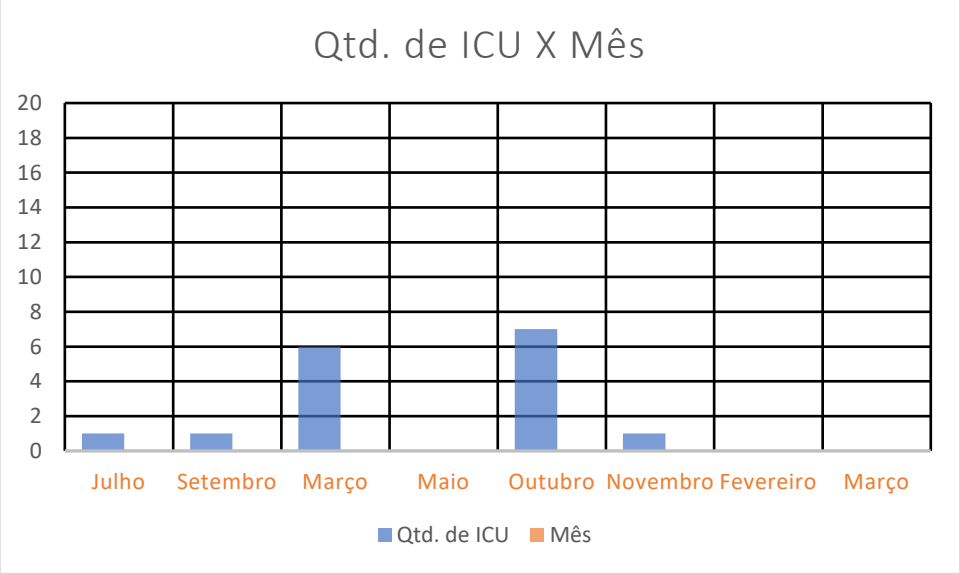

Source: Prepared by the author.

Chart 3: Comparative Chart of the ICU for the year 2020

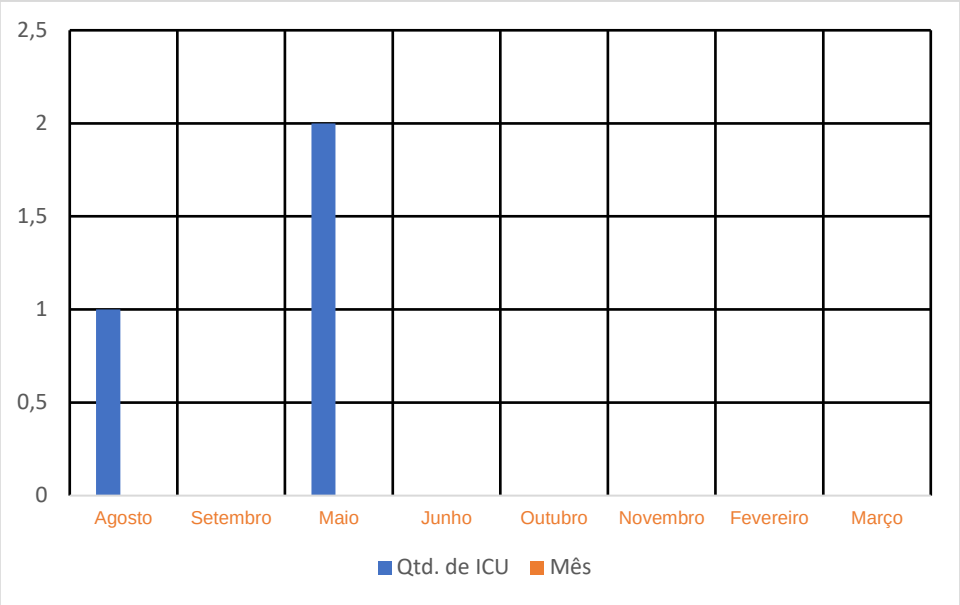

Source: Prepared by the author.

Chart 4: Comparative Chart of the ICU for the year 2021

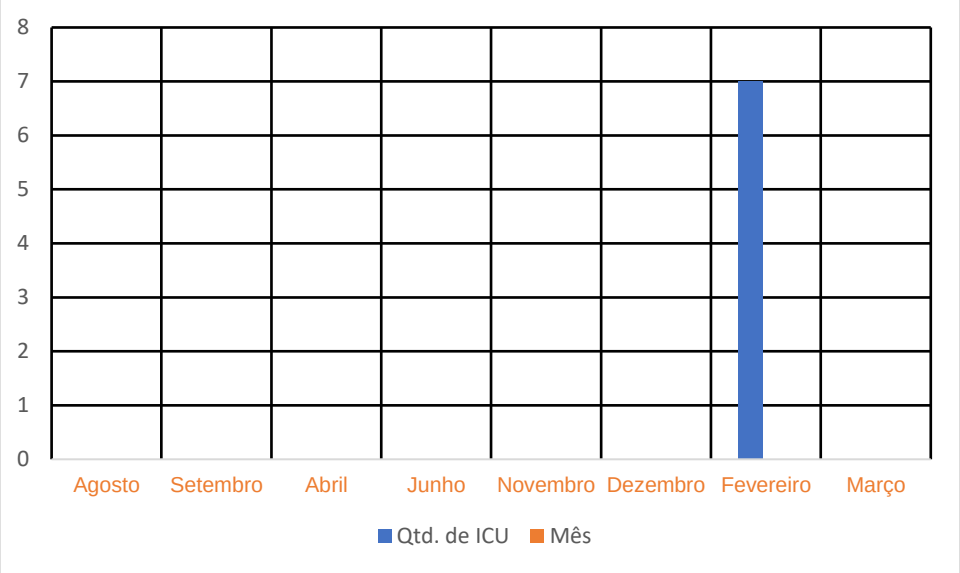

Source: Prepared by the author.

DEDICATION

I dedicate this work:

To my parents Edelves and Flávio who always supported me in my decisions and who always helped me, to my brothers Beatriz and Mateus who have always been my source of emotional support.

ACKNOWLEDGMENT

To my friends Rodrigo, Nitah, Norris, Naty, Giovanny and so many others who helped me during my graduation.

I would like to thank my "brothers" Brendow, Flavinho and Dara who even from afar always cheered for my success.

I would also like to thank my great advisor Helio Ricardo who was like a second father to me during graduation, always helping me and encouraging me to achieve my goals.

I would also like to thank the Academic Athletic Association of Ilha Solteira, where I had the opportunity to learn more about myself, I lived unforgettable moments with the staff and I would like to thank especially Daniel (Boladona), who always encouraged me to do things right.

And lastly the BIOMAS Junior Company, where I met wonderful people who taught me the meaning of teamwork, I would like to especially thank Lana Avelar, who supported me within the enterprise pointing out my mistakes and defects. And also to Pedro Oliveira and Caroline who encouraged me to participate in the selection processes

REFERENCES

ABREU, K. M. P; COUTINHO, L. M. Sensoriamento remoto aplicado ao estudo da vegetação com ênfase em índice de vegetação e métricas da paisagem. VÉRTICES, Campos dos Goytacazes/RJ, v.16, n.1, p. 173-198, jan. /abr. 2014

AMORIM, M. C. C. T.; DUBREUIL, V. Intensity of Urban Heat Islands in Tropical and Temperate Climates. Climate, v.5, p.91 - 104, 2017.

AYOADE, J. O. Introdução à climatologia para os trópicos. 11º ed. - Rio de Janeiro: Bertrand, Brasil, 2006. 332p.

BARBOSA, R. V. R.; VECCHIA, F. A. S. "Estudos de Ilha de Calor Urbana por meio de Imagens do Landsat 7 Etm+: Estudo de Caso em São Carlos (SP)". Revista Minerva – Pesquisa e Tecnologia, v. 6, n. 3, set. /dez. 2009. Disponível em: Acesso em: 17 dez. de 2021.

BARROS, M. P. Dimensão fractal e ilhas de calor urbanas: uma abordagem sistêmica sobre as implicações entre a fragmentação das áreas verdes e o ambiente térmico do espaço urbano. 2012. 210 f. Tese (Doutorado em Física Ambiental) - Universidade Federal de Mato Grosso, Cuiabá, 2012.

CDC – CENTER FOR DISEASE CONTROL AND PREVENTION. Heat-Related Deaths – Unitted States, 1993-2003. 2004. Morbidity and Mortality Weekly Report. Disponivel em: < http://www.cdc.gov/mmwr/preview/mmwrhtml/mm5529a2. htm>. Acesso em 19 dez 2021.

COLTRI, P.P. Influência do uso e cobertura do solo no clima de Piracicaba, São Paulo: análise de séries históricas, ilhas de calor e técnicas de sensoriamento remoto. 2006. 166p.Dissertação (Mestrado em Fitotecnia) – Escola Superior de Agricultura "Luiz de Queiroz", Universidade de São Paulo, Piracicaba. 2006.

CORRÊA, P.B.et al. Heat Island in Manaus city: study with remote sensing Data, Modeling and Meteoroligical Data. Revista Brasileira de Meteorologia, São José dos Campos, v. 31, n. 2, p. 167-176, 2016.

COSTA, D. F.; SILVA, H. R.; PERES, L. F. Identificação de ilhas de calor na área urbana de Ilha Solteira-SP através da utilização de geotecnologias. Engenharia Agrícola, Jaboticabal, v. 30, n. 5, p. 974-985, 2010.

GAMARRA, N. L. R.; CORRÊA, M. P.; TARGINO, A. C. L. Utilização de sensoriamento remoto em análises de albedo e temperatura de superfície em Londrina–PR: contribuições para estudos de ilha de calor urbano. Revista Brasileira de Meteorologia, São José dos Campos, v. 29, n. 4, p. 537-550, 2014. Disponível em: < http://www.scielo.br/pdf/rbmet/v29n4/07.pdf>. Acesso em: 12 dez. 2021.

GARCÍA, F. F. Manual de climatología aplica: clima, medio ambiente y planificación. Madrid: Editorial Síntesis, 1996. 285 p.

GARTLAND, L. Ilhas de calor: como mitigar zonas de calor em áreas urbanas. São Paulo: Oficina de Textos, 2010.

GIORDANO, D. E.; KRÜGER, E. L. Potencial de redução da temperatura de superfície pelo aumento do albedo nas diversas regiões brasileiras. Paranoá: cadernos de arquitetura e urbanismo, Brasília, DF, n. 11, p. 13-22, 2014. Disponível em:< http://periodicos.unb.br/index.php/paranoa/article/view/12080/8465>. Acesso em: 16 dez. 2021.

GOMES BRASILEIRO, F. M.; ZANELLA, M. E. Occurrence of heat islands in urban space: reflections in the context of the city of Sobral, Ceará. Geopauta, *[S. l.]*, v. 5, n. 4, p. e9499, 2021. DOI: 10.22481/rg. v5i4.e2021.e9499. Disponível em: https://periodicos2.uesb.br/index.php/geo/article/view/9499. Acesso em: 9 feb. 2022.

Hernandez, F.B.T. Análise agroclimática da área de influência do Reservatório da Usina Hidrelétrica de Ilha Solteira, região noroeste do Estado de São Paulo. Ilha Solteira: UNESP, FEPISA e SEAP/PR (Convênio 80/2005), 2007. 27 p.

HU, Y.; JIA, G. Influence of land use change on urban heat island derived from multi-sensor data. International Journal of Climatology, Chichester, v. 30, n. 9, p. 1382 - 1395, 2010.

IBGE. Instituto Brasileiro de Geografia e Estatística. Perfil dos municípios brasileiros. IBGE, Coordenação de População e Indicadores Sociais, Rio de Janeiro. 2017.

INSTITUTO BRASILEIRO DE GEOGRAFIA E ESTATÍSTICA - IBGE. Cidades: 2010, Censo demográfico. Disponível em: https://cidades.ibge.gov.br. Acesso em: 18 dez. 2021.

KEGLER, J. J.; WOLLMANN, C. A.; BANDEIRA, B. C. O SISTEMA TERMODINÂMICO DE CIDADES PEQUENAS: CONFIGURAÇÃO URBANO-RURAL COM USO DE TRANSECTOS MÓVEIS EM AGUDO/RS, SITUAÇÃO VERANIL DE JANEIRO DE 2016. Caminhos de Geografia, [S. l.], v. 18, n. 62, p. 32–48, 2017. Disponível em: https://seer.ufu.br/index.php/caminhosdegeografia/article/view/34799. Acesso em: 18 dez. 2021.

LANDSBERG, H. E The Climate of towns. In: LANDSBERG Man's role in changing the face of Earth. Chicago: The Wenner Grem Foundation Antropological Research. The University of Chicago Press, 2006. p. 10-15

MASHIKI, M. Y. Geoprocessamento na identificação de ilhas de calor e influência do uso e ocupação do solo na temperatura aparente da superfície no município de Botucatu/SP. 2012. Dissertação (Mestrado em Agronomia) – Faculdade de Ciências Agronômicas, Universidade Estadual Paulista, Botucatu, 2012.

MENDONÇA, F.; DANNI-OLIVEIRA, I. M. Climatologia noções básicas e climas do Brasil. Ed. Oficina de Textos. São Paulo. 2007. 206p.

MENESES, P. R; ALMEIDA, T. Introdução ao processamento de imagens de sensoriamento remoto. Brasília: Universidade de Brasília –UNB, 2012.

MORAES, E. C. Fundamentos de Sensoriamento Remoto. São José dos Campos –SP: INPE, 2002. Capítulo 1.

MOREIRA, J. C.; SENE, E. Geografia Geral e do Brasil: espaço geográfico e globalização. 2. ed. São Paulo: Scipione, 2004. 275 p.

NAKATA-OSAKI, Camila Mayumi e SOUZA, Léa Cristina Lucas De e RODRIGUES, Daniel Souto. Impacto da geometria do cânion urbano na intensidade de ilha de calor noturna: análise através de um modelo simplificado adaptado a um SIG. Ambiente Construído, v. 16, n. 3, p. 73–87, 2016.

Organização das Nações Unidas (ONU). Disponível em: https://news.un.org/pt/story/2017/06/1589091-populacao-mundial-atingiu-76-bilhoes-de-habitantes. Acessado em/18/12/2021

PARANHOS-FILHO, A. C; LASTORIA, G; TORRES, T. G. Sensoriamento Remoto ambiental aplicado: Introdução as Geotecnologias. Ed. UFMS, Campo Grande/MS, 2008.

POPULATION BULLETIN. Word Population Highlights: Key findings from PRB's 2007 World population data sheet. Population Reference Bureau. v. 62, nº 3, 2007. Disponível em: https://assets.prb.org. Acesso em: 18 dez. 2021.

PORANGABA, Gislene Figueiredo Ortiz e AMORIM, Margarete Cristiane de Costa Trindade. Geotecnologias Aplicadas à Análise de Ilhas de Calor de Superfície em Cidades do Interior do Estado de São Paulo. Revista Brasileira de Geografia Física, v. 12, n. 6, p. 2041, 2019.

PRB (Population Reference Bureau). Disponível em: www.prb.org> acessado em 18 dez. 2021

RIBEIRO, Helena e PESQUERO, Célia Regina e DE SOUSA ZANOTTI STAGLIORO COELHO, Micheline. Clima urbano e saúde: Uma revisão sistematizada da literatura recente. Estudos Avançados, v. 30, n. 86, p. 67-85, 2016

ROTH, M. Urban heat islands. Handbook of environmental fluid dynamics. Volume two: systems, pollution, modeling, and measurements. CRC Press, Boca Raton, FL, p. 143-160, 2013.

SAYDELLES, A. P. Estudo do campo térmico e das ilhas de calor urbano em Santa Maria - RS. 2005. 219f. Dissertação (Dissertação de mestrado) – Universidade Federal de Santa Maria, 2005. Disponível em: Acesso em: 17. dez. de 2021.

THE WORLD BANK. Urban Development. Disponível em: <http://www.worldbank.org/en/topic/urbandevelopment/overview>. Acesso em: 18 fev. 2021.

VOOGT, J. A.; OKE, T. R. Thermal remote sensing of urban climates. Remote Sensing of Environment, New York, v. 86, p. 370-384, 2003.